
Dimension-Free Multimodal Sampling via Preconditioned Annealed Langevin Dynamics

Lorenzo Baldassari¹ Josselin Garnier² Knut Sølna³ Maarten V. de Hoop⁴

Abstract

Designing algorithms that can explore multimodal target distributions accurately across successive refinements of an underlying high-dimensional problem is a central challenge in sampling. Annealed Langevin dynamics (ALD) is a widely used alternative to classical Langevin since it often yields much faster mixing on multimodal targets, but there is still a gap between this empirical success and existing theory: when, and under which design choices, can ALD be guaranteed to remain stable as dimension increases? In this paper, we help bridge this gap by providing a uniform-in-dimension analysis of continuous-time ALD for multimodal targets that can be well-approximated by Gaussian mixture models. Along an explicit annealing path obtained by progressively removing Gaussian smoothing of the target, we identify sufficient spectral conditions—linking smoothing covariance and the covariances of the Gaussian components of the mixture—under which ALD achieves a prescribed accuracy within a single, dimension-uniform time horizon. We then establish dimension-robustness to imperfect initialization and score approximation: under a misspecified-mixture score model, we derive explicit conditions showing that preconditioning the ALD algorithm with a sufficiently decaying spectrum is necessary to prevent error terms from accumulating across coordinates and destroying dimension-uniform control. Finally, numerical experiments illustrate and validate the theory.

1. Introduction

Classical Langevin dynamics is a standard tool for sampling (Parisi, 1981; Roberts & Tweedie, 1996; Roberts & Rosenthal, 1998) and a key ingredient in recent score-based

¹University of Basel ²Ecole Polytechnique, IP Paris ³University of California Irvine ⁴Rice University. Correspondence to: Lorenzo Baldassari <lorenzo.baldassari@unibas.ch>.

Preprint. February 3, 2026.

generative models (Song & Ermon, 2019; Song et al., 2021). Its limitations, however, are also well known. While it can converge rapidly when the target distribution is strongly log-concave or satisfies suitable isoperimetric inequalities (Durmus et al., 2019; Vempala & Wibisono, 2019; Chewi et al., 2025), its behavior can deteriorate dramatically outside these regimes: for non-strongly log-concave and especially multimodal distributions, its mixing can be extremely slow, and this difficulty typically becomes more severe as the dimension increases (Ma et al., 2019; Schlichting, 2019; Dong & Tong, 2022). Rigorous results confirm such failures in a variety of scenarios, including Bayesian posteriors in nonlinear inverse problems (Bohr & Nickl, 2024; Bandeira et al., 2023; Nickl, 2023).

These challenges have led to annealed Langevin dynamics (ALD). Building on the empirical success of annealing-based strategies (Kirkpatrick et al., 1983; Gelfand & Mitter, 1990; Neal, 2001), the ALD scheme considered here simulates Langevin dynamics starting from a heavily regularized (hence easier-to-sample) distribution and then gradually reduces the smoothing until it approaches the desired target (Song & Ermon, 2019; Block et al., 2020). ALD is often reported to improve exploration across modes and to yield substantially better finite-time sampling accuracy (Song & Ermon, 2020; Zilberstein et al., 2022; Sun et al., 2024), and recent theoretical work has begun to clarify why annealing can outperform classical Langevin under minimal assumptions—sometimes turning worst-case sampling complexity upper bounds from exponential to polynomial (Guo et al., 2025). Nevertheless, important questions remain open—especially whether sampling can remain uniformly stable as the dimension increases, without incurring substantially longer mixing times. This question has been the object of many studies for classical Langevin (Cotter et al., 2013; Durmus et al., 2017), but has not yet been rigorously addressed for ALD, except under strong regularity assumptions on the target distribution (Cattiaux et al., 2025). Yet robustness is most critical in multimodal regimes, where classical Langevin can fail.

A simple illustration suggests that this goal may not be out of reach. Figure 1 considers, for each dimension d , sampling from a bimodal Gaussian mixture on \mathbb{R}^d with weights

$(w_1, w_2) = (0.75, 0.25)$, means $(0, 10e_1)$, and covariances $\tau_1 \Sigma^d$ and $\tau_2 \Sigma^d$, where $\tau_1 = 1.2$, $\tau_2 = 2$, and Σ^d has a decaying spectrum $(j^{-2})_{j=1}^d$. Fixing $\epsilon = 0.3$, we ask whether the number of ALD steps needed to reach this accuracy grows with d . The target is clearly multimodal, and even for moderate dimensions ALD already exhibits a pronounced dependence on d , in line with existing pessimistic bounds (Guo et al., 2025); for $d > 10$ the required number of steps exceeds our 20000-step cap. However, under a few specific *design choices*—like changing the spectrum of the smoothing operator from flat to sufficiently decaying—ALD reaches the prescribed accuracy with no visible deterioration in the required number of steps.

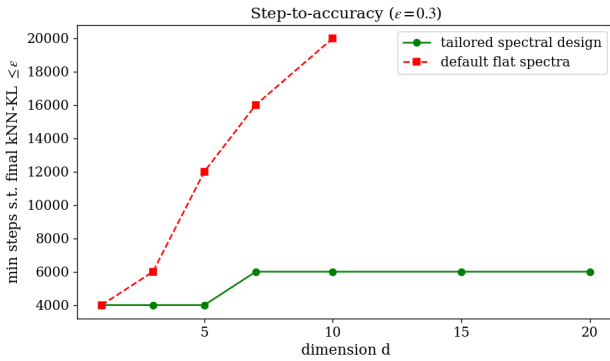


Figure 1. ALD step count vs. dimension. Number of ALD time steps required for the empirical $\text{KL}(\rho_*^d \parallel \rho^{\text{ALD}, d})$ to fall below the prescribed accuracy $\epsilon = 0.3$, plotted against the truncation dimension d . The red curve corresponds to the default flat-spectrum choice, with preconditioner $\Gamma = I$ and smoothing $C = 40I$, while the green curve corresponds to a tailored spectral design: $\Gamma = \text{Diag}(j^{-1.5})_{j \geq 1}$ and $C = \text{Diag}(40 \cdot j^{-2.7})_{j \geq 1}$.

Despite being only illustrative, this toy example highlights a gap between existing theory—where current results typically suggest that finite-time sampling accuracy deteriorates with dimension at a polynomial rate (Guo et al., 2025)—and the empirical behavior observed here. This motivates the central question of this theoretical paper: *can one design meaningful annealed Langevin configurations for which stable sampling in high dimensions is not only within reach, but can also be explained rigorously?* The main message of this work is that it is possible. Specifically, we identify a physically motivated ALD design that yields *dimension-uniform* sampling guarantees for multimodal distributions in continuous time (Section 3), and we derive conditions under which these guarantees remain stable under score and initialization errors (Section 4). A key conclusion is that stability is not automatic: as we show in subsection 4.2, it requires appropriate preconditioning of the ALD diffusion.

Our analysis is carried out for Gaussian mixture models (GMMs), a classical and widely used family for approximating complex distributions (McLachlan & Peel, 2000). For

each dimension d , we consider targets of the form

$$\rho_*^d = \sum_{i \in I} w_i \mathcal{N}(m_i^d, \Sigma_i^d),$$

where I may be finite or countably infinite, the weights satisfy $w_i > 0$ and $\sum_{i \in I} w_i = 1$, and (m_i^d, Σ_i^d) denote the component means and covariances in \mathbb{R}^d . We view the family $(\rho_*^d)_{d \geq 1}$ as a sequence of increasingly accurate finite-dimensional models—obtained, for example, by projecting an infinite-dimensional target onto its first d coordinates (see Section 2)—and we analyze whether ALD can achieve controlled sampling accuracy uniformly in d as the truncation level increases. This setting is general yet tractable: it lets us make explicit how the annealing schedule, the preconditioner, and the mixture geometry (means, covariances, and weights) jointly yield dimension-uniform guarantees for the continuous-time ALD diffusion, together with conditions ensuring stability under score and initialization mismatch. These insights translate into concrete design choices, illustrated numerically in Section 5; while we do not provide a discretization analysis here, our results nonetheless suggest principled guidelines for practice.

Related Work

Our work is primarily motivated by the recent wave of papers focusing on infinite-dimensional analyses for diffusion/score-based generative models (Kerrigan et al., 2023; Franzese et al., 2023; Baldassari et al., 2023; Pidstrigach et al., 2024; Bond-Taylor & Willcocks, 2024; Baldassari et al., 2024; Lim et al., 2025; Hagemann et al., 2025; Baldassari et al., 2025; Franzese & Michiardi, 2025), and by the limitations of these results when the target distribution becomes multimodal.

Non-asymptotic analyses of Langevin-type samplers are well developed under strong regularity assumptions (e.g. strong log-concavity), where one can obtain sharp guarantees on mixing and discretization error (Dalalyan, 2017; Durmus et al., 2017; 2019; Vempala & Wibisono, 2019; Chewi et al., 2025). These analyses also highlight a key limitation: for multimodal targets, comparable guarantees for classical Langevin are typically out of reach, since metastability and energy barriers dominate the mixing behavior (Ma et al., 2019; Schlichting, 2019; Dong & Tong, 2022).

Motivated by this difficulty, annealing-based strategies alter the sampling task through a prescribed path of intermediate distributions that progressively flattens the landscape (Kirkpatrick et al., 1983; Gelfand & Mitter, 1990; Neal, 2001). Evolving a Langevin diffusion along these schedules leads to annealed Langevin dynamics (Cattiaux et al., 2025). While early uses of ALD were largely heuristic (Song & Ermon, 2019; 2020), more recent theory—driven in part by the popularity of *stochastic interpolants* (Albergo

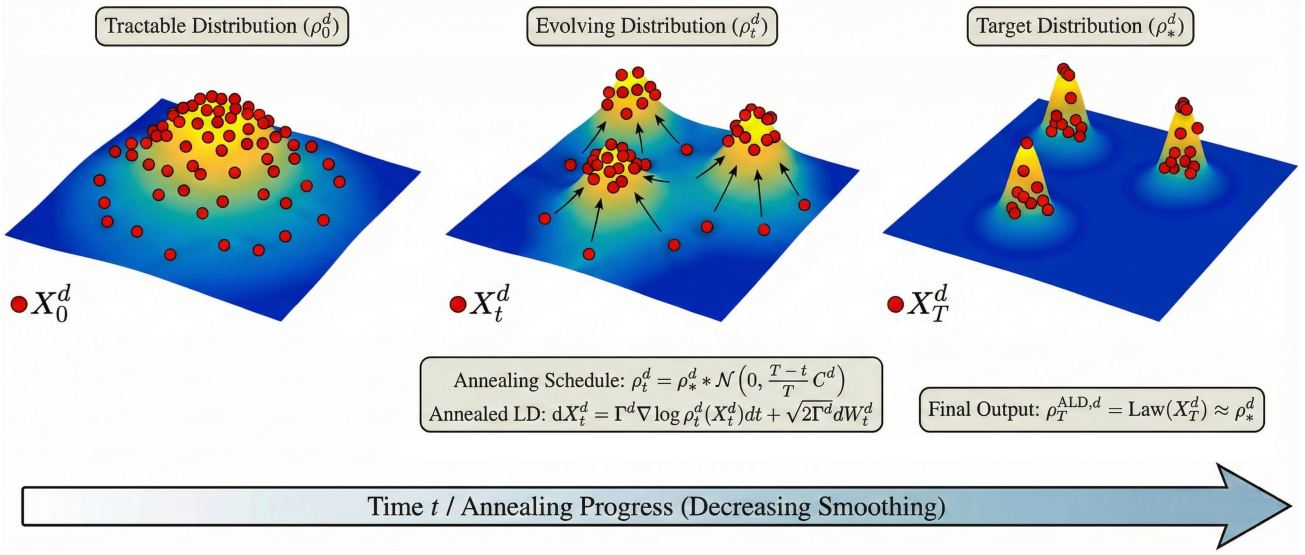


Figure 2. Illustration of annealed Langevin dynamics. The ALD scheme considered here starts from a heavily smoothed, and hence tractable, version of the target and simulates a Langevin diffusion whose drift is adapted to the current smoothing level. As time progresses, the smoothing is gradually removed, so the dynamics moves from an almost unimodal distribution back to the original multimodal target through a controlled ‘‘complexification’’ of the landscape.

et al., 2025), which can be viewed as a generalization of ALD (Cordero-Encinar et al., 2025)—has renewed interest in samplers based on diffusion dynamics with prescribed, time-dependent score schedules. A particularly interesting example in conditional generation, which we discuss in Appendix C, is *classifier-free guidance* (Pavasovic et al., 2025; Yehezkel et al., 2025; Wang et al., 2024), where the sampling score is formed by combining conditional and unconditional scores with a guidance weight that is often taken to be time-dependent (stronger early and tapered later).

Our contribution is in the same vein as this growing body of work, but with one important difference: by foregrounding robustness with respect to dimension, we consider a family of truncations of an *infinite-dimensional multimodal model*, and we make explicit how dimension-robustness can be enforced through the spectral properties of both the annealing geometry and the preconditioner. This perspective connects naturally to the function-space MCMC literature, which has long emphasized that Langevin-type algorithms should be formulated in infinite dimension *before* discretization; doing so makes it possible to design principled preconditioning schemes that yield dimension-independent behavior (Cotter et al., 2013; Hairer et al., 2014; Cui et al., 2016; Beskos et al., 2017). It is also in this sense that, as mentioned at the beginning of this section, our work can be viewed as parallel to recent analyses of preconditioned score-based generative models (Pidstrigach et al., 2024; Baldassari et al., 2025).

2. Problem Setting

Our goal is to understand when continuous-time annealed Langevin dynamics can sample *robustly across the successive refinements* $(\rho_*^d)_{d \geq 1}$ of an infinite-dimensional multimodal target distribution ρ_*^∞ . As d grows—resolving progressively finer features of the same target—we ask whether (i) a single, *fixed* time horizon can control the sampling error uniformly in d when the annealing scores are available exactly, and (ii) whether the procedure remains stable under approximation errors and imperfect initialization.

To make these questions precise, we first formalize the infinite-dimensional setting, which fixes both the modeling assumptions and the notion of refinement used throughout the paper. Let H be a separable Hilbert space with orthonormal basis $(e_j)_{j \geq 1}$. We consider a Gaussian mixture on H ,

$$\rho_*^\infty = \sum_{i \in I} w_i \mathcal{N}(m_i, \Sigma_i),$$

where I is finite or countably infinite, $w_i > 0$ for all $i \in I$, and $\sum_{i \in I} w_i = 1$. We focus on a diagonal setting:

$$m_i = \sum_{j \geq 1} m_{ij} e_j, \quad \Sigma_i e_j = \sigma_{ij} e_j, \quad \sigma_{ij} > 0.$$

Assumption 2.1 (Finite-energy). *For each component $i \in I$ of $\rho_*^\infty = \sum_{i \in I} w_i \mathcal{N}(m_i, \Sigma_i)$,*

$$\sum_{j \geq 1} m_{ij}^2 < \infty, \quad \sum_{j \geq 1} \sigma_{ij} < \infty.$$

Note that Assumption 2.1 is not an *ad hoc* hypothesis: it is the Hilbert-space analogue of finite energy. In other words, it guarantees $m_i \in H$ and that Σ_i are trace-class, so that each $\mathcal{N}(m_i, \Sigma_i)$ is a well-defined Gaussian measure on H (Hairer, 2009).

The next step, preceding our analysis of ALD, is the definition of the finite-dimensional targets via truncation. Let P_d be the orthogonal projection onto $\text{span}\{e_1, \dots, e_d\}$. The d -dimensional target is the marginal

$$\rho_*^d := (P_d)_\# \rho_*^\infty = \sum_{i \in I} w_i \mathcal{N}(m_i^d, \Sigma_i^d), \quad (1)$$

where

$$m_i^d = (m_{i1}, \dots, m_{id}), \quad \Sigma_i^d = \text{Diag}(\sigma_{i1}, \dots, \sigma_{id}).$$

Thus, increasing d adds new modes governed by the same spectral sequences, while leaving the previously defined coordinates unchanged. This is the refinement regime in which we seek dimension-uniform guarantees.

3. Annealed Langevin Dynamics

The targets ρ_*^d are multimodal, and classical Langevin dynamics is well known to struggle with multimodal sampling even at moderate dimension. In this section, we introduce one possible remedy—annealed Langevin dynamics (ALD)—which simulates a Langevin diffusion along a prescribed sequence of progressively less smoothed targets. Here we focus on the Gaussian-smoothing variant of ALD; it is sketched in Figure 2 and formalized below in two steps.

Step 1 (annealing schedule). Let C^d be a positive-definite matrix, diagonal in the basis $(e_j)_{j=1}^d$ with eigenvalues $(\lambda_j)_{j=1}^d$. To remain consistent with the infinite-dimensional setting, we assume the eigenvalues are the first d terms of a summable sequence $(\lambda_j)_{j \geq 1}$, i.e.,

$$\sum_{j \geq 1} \lambda_j < \infty, \quad (2)$$

so that the limiting covariance on H is trace-class. We define the Gaussian-smoothing annealing path by

$$\rho_t^d = \rho_*^d * \mathcal{N}\left(0, \frac{T-t}{T} C^d\right), \quad t \in [0, T]. \quad (3)$$

Thus, at early times ($t \approx 0$), ρ_t^d is a heavily smoothed version of ρ_*^d , and is typically easier to explore; as $t \rightarrow T$, the smoothing vanishes and ρ_t^d returns to the original multimodal target.

Step 2 (time-inhomogeneous dynamics). We then define a diffusion driven by a time-dependent score $\nabla \log \rho_t^d$: starting from ρ_0^d , the dynamics is gradually driven toward the

target $\rho_T^d = \rho_*^d$. Specifically, we initialize $X_0^d \sim \rho_0^d$ and evolve the ALD diffusion

$$dX_t^d = \Gamma^d \nabla \log \rho_t^d(X_t^d) dt + \sqrt{2\Gamma^d} dW_t^d, \quad t \in [0, T], \quad (4)$$

where $(W_t^d)_{t \geq 0}$ is a standard Brownian motion in \mathbb{R}^d , and Γ^d is a positive-definite matrix, also diagonal in the basis $(e_j)_{j=1}^d$ with eigenvalues $(\gamma_j)_{j=1}^d$, whose role as a preconditioner will be discussed later. The corresponding ALD output distribution, which we use as an *approximation* of ρ_*^d , is the law at time T

$$\rho_T^{\text{ALD}, d} := \text{Law}(X_T^d). \quad (5)$$

There is an important distinction to keep in mind, which helps clarify the analysis that follows. Standard Langevin dynamics targeting ρ_*^d uses a fixed drift, $\nabla \log \rho_*^d$. In contrast, ALD uses the time-dependent score $\nabla \log \rho_t^d$, so the dynamics (4) is time-inhomogeneous. Consequently, one should not expect a stationary distribution, nor should one expect the law $\rho_t^{\text{ALD}, d} := \text{Law}(X_t^d)$ to coincide with the instantaneous target ρ_t^d ; in fact, $\rho_T^{\text{ALD}, d}$ may differ from ρ_*^d . We quantify this *annealing-induced bias* at the final time T via the Kullback-Leibler divergence

$$\mathcal{B}_{\text{ann}}^d(T) := \text{KL}(\rho_*^d \parallel \rho_T^{\text{ALD}, d}).$$

In what follows, we show that the time T required to make this bias small is dictated by the schedule and by the geometry of smoothing and preconditioning (through C^d and Γ^d), as well as by the mixture covariances (Σ_i^d) ; with the right design choice, it can be made *uniform in dimension*.

Annealing-Induced Bias

To isolate the source of this bias, it is convenient to introduce a reference time-inhomogeneous diffusion that *does* follow the annealing path exactly. Namely, we consider a time-dependent vector field $(v_t^d)_{t \in [0, T]}$ and the SDE

$$dX_t^d = \Gamma^d (\nabla \log \rho_t^d + v_t^d)(X_t^d) dt + \sqrt{2\Gamma^d} dW_t^d, \quad (6)$$

with v_t^d chosen so that $\text{Law}(X_t^d) = \rho_t^d$ for all $t \in [0, T]$. In particular, any such v_t^d induces the path-matching energy,

$$\mathcal{J}_{\text{ann}}^{v_t^d}(T) := \frac{1}{4} \int_0^T \int_{\mathbb{R}^d} \|(\Gamma^d)^{1/2} v_t^d(x)\|^2 d\rho_t^d(x) dt, \quad (7)$$

(with a slight abuse of notation, we use ρ_t^d both for the law and for its density), which upper bounds $\mathcal{B}_{\text{ann}}^d(T)$ for any v_t^d . In other words, controlling the bias reduces to controlling the energy cost of the correction v_t^d needed to match the annealing path, relative to the *cheap* drift $\nabla \log \rho_t^d$ used by the ALD diffusion (4). This is not merely a technical convenience: in general, v_t^d is inaccessible, since identifying it amounts to solving a high-dimensional Fokker-Planck

equation. Although for Gaussian mixtures such corrections can sometimes be characterized explicitly, we adopt this setting as a tractable proxy in which all quantities are explicit and the dependence on (C^d, Γ^d) and (Σ_i^d) can be tracked.

This leads to the paper's first question: *how large must the annealing horizon be* so that this bias stays within a prescribed accuracy ϵ ? In particular, how does the required time horizon scale with the dimension d ? Theorem 3.1 below answers this by giving a time horizon T^d such that

$$\text{KL}(\rho_\star^d \| \rho_{T^d}^{\text{ALD},d}) \leq \epsilon,$$

with T^d depending on d only via (λ_j, γ_j) and (σ_{ij}) . We then use this dimension-explicit expression for T^d to identify regimes in which achieving accuracy ϵ requires a time horizon can be chosen uniformly in d . The result is proved in Appendix A under exact-score and perfect-initialization assumptions; we relax both in the next section.

Theorem 3.1. *Fix $d \geq 1$ and $\epsilon > 0$. Define*

$$\mathcal{K}_d := \frac{1}{16} \sum_{i \in I} w_i \sum_{j=1}^d \frac{\lambda_j}{\gamma_j} \log\left(1 + \frac{\lambda_j}{\sigma_{ij}}\right).$$

Consider the ALD dynamics up to time

$$T^d := \epsilon^{-1} \mathcal{K}_d.$$

Then $\mathcal{B}_{\text{ann}}^d(T^d) \leq \epsilon$.

Theorem 3.1 shows that a dimension-uniform horizon exists precisely when $\sup_{d \geq 1} \mathcal{K}_d < \infty$, that is, when the series

$$\sum_{i \in I} w_i \sum_{j \geq 1} \frac{\lambda_j}{\gamma_j} \log\left(1 + \frac{\lambda_j}{\sigma_{ij}}\right)$$

is finite. In such regimes, the required time horizon to reach accuracy ϵ does not deteriorate as d increases, formalizing the dimension-stability suggested by Figure 1. Crucially, this condition can be enforced through *design choices* in ALD, namely by selecting the spectrum (λ_j) of the Gaussian-smoothing covariance and the preconditioner spectrum (γ_j) : indeed, using $\log(1 + u) \leq u$ for $u \geq 0$, a sufficient condition for $\sup_d \mathcal{K}_d < \infty$ is

$$\sum_{i \in I} w_i \sum_{j \geq 1} \frac{\lambda_j^2}{\gamma_j \sigma_{ij}} < \infty. \quad (8)$$

Finally, three remarks are worth noting:

- It may seem surprising that the component means m_{ij} do not appear in (8). This is because Theorem 3.1 assumes an idealized setting; in the next section we show that the means m_{ij} play a significant role when the score is imperfect or the initialization is misspecified.

- Theorem 3.1 assumes access to an exact initialization $X_0^d \sim \rho_0^d$; it does not quantify the cost of sampling from ρ_0^d . This cost is controlled by the smoothing C^d , which, when increased, makes $\rho_0^d = \rho_\star^d * \mathcal{N}(0, C^d)$ closer to a unimodal proxy and typically easier to sample from, but also increases \mathcal{K}_d since the annealing path starts farther from ρ_0^d . Conversely, weaker smoothing shortens the path but yields a more multimodal ρ_0^d , which is harder to sample from.
- One should not read the dependence of \mathcal{K}_d on (γ_j) as saying that multiplying Γ^d by a large scalar accelerates sampling: this operation essentially rescales the continuous-time clock (e.g. when $\Gamma^d = \kappa C^d$, only $T' = \kappa T$ becomes meaningful), and in discrete time it demands a correspondingly smaller stepsize to remain stable. What matters for dimension-free control is the *spectral shape* of Γ^d relative to C^d , a point that becomes especially important in the next section when score and initialization errors are included.

4. Dimension-Robust Sampling under Score and Initialization Errors

We now move past the idealized setting of Section 3 and turn to the question of *dimension-uniform stability* when the continuous-time dynamics evolves under an imperfect score and a misspecified initialization. To separate the contribution of these errors from the intrinsic annealing-induced bias analyzed in the previous section, we keep the ideal annealing diffusion (6) as a reference and compare it to the practical ALD driven by an approximate score and started from an incorrect initial law:

$$d\tilde{X}_t^d = \Gamma^d s_\theta^d(t, \tilde{X}_t^d) dt + \sqrt{2\Gamma^d} d\tilde{W}_t^d, \quad \tilde{X}_0^d \sim \tilde{\rho}_0^d. \quad (9)$$

We denote its law by $\tilde{\rho}_t^{\text{ALD},d} := \text{Law}(\tilde{X}_t^d)$ (recall that the ALD law with exact score is denoted by $\rho_t^{\text{ALD},d}$), and we measure score inaccuracies through the pointwise error

$$\epsilon_t^d(x) := \nabla \log \rho_t^d(x) - s_\theta^d(t, x).$$

We start our analysis with the following proposition, whose proof is given in Appendix B.1.

Proposition 4.1. *We have the upper bound*

$$\text{KL}(\rho_\star^d \| \tilde{\rho}_T^{\text{ALD},d}) \leq \mathcal{E}_{\text{init}}^d + \mathcal{E}_{\text{score},T}^d + \mathcal{E}_{\text{bias},T}^d, \quad (10)$$

where

$$\mathcal{E}_{\text{init}}^d := \text{KL}(\rho_0^d \| \tilde{\rho}_0^d),$$

$$\mathcal{E}_{\text{score},T}^d := \frac{1}{2} \int_0^T \int \left\| (\Gamma^d)^{1/2} \epsilon_t^d(x) \right\|^2 d\rho_t^d(x) dt,$$

and

$$\mathcal{E}_{\text{bias},T}^d := 2 \inf_{\substack{(v_t^d)_{t \in [0,T]}: \\ \partial_t \rho_t^d = -\nabla \cdot (\rho_t^d \Gamma^d v_t^d)}} \mathcal{J}_{\text{ann}}^{v_t^d}(T),$$

with $\mathcal{J}_{\text{ann}}^{v^d}(T)$ defined in (7).

Note that Theorem 3.1 already provides a dimension-explicit bound for $\mathcal{E}_{\text{bias},T}^d$. Indeed, the argument underlying (10) relies on the inequality

$$\mathcal{B}_{\text{ann}}^d(T) \leq \frac{1}{2} \mathcal{E}_{\text{bias},T}^d,$$

and Theorem 3.1 bounds this path-matching energy through the same quantity \mathcal{K}_d . In particular, the dimension-uniform regimes identified there—namely, the sufficient condition (8)—apply directly to $\mathcal{E}_{\text{bias},T}^d$. It therefore remains to control the terms $\mathcal{E}_{\text{init}}^d$ and $\mathcal{E}_{\text{score},T}^d$, which we do next. To this end, we introduce a score-error model that keeps the analysis explicit while preserving multimodality.

Assumption 4.2. *The learned score coincides with the exact score of a misspecified Gaussian mixture along the annealing path:*

$$s_{\theta}^d(t, x) = \nabla \log \tilde{\rho}_t^d(x),$$

where $\tilde{\rho}_t^d$ is obtained by annealing a perturbed mixture with the same smoothing operator as in (3), namely

$$\tilde{\rho}_t^d = \tilde{\rho}_{\star}^d * \mathcal{N}\left(0, \frac{T-t}{T} C^d\right), \quad \tilde{\rho}_{\star}^d := \sum_{i \in I} \tilde{w}_i \mathcal{N}(\tilde{m}_i^d, \tilde{\Sigma}_i^d),$$

with perturbed parameters

$$\tilde{m}_i^d = m_i^d + \Delta m_i^d, \quad \tilde{\Sigma}_i^d = \Sigma_i^d + \Delta \Sigma_i^d, \quad \tilde{w}_i = w_i + \Delta w_i,$$

and with $(\tilde{w}_i)_{i \in I}$ such that $\tilde{w}_i > 0$ and $\sum_{i \in I} \tilde{w}_i = 1$.

For the calculations that follow we continue adopting the diagonal setting introduced in Section 2: in particular, we assume that, for each d and each $i \in I$,

$$\Delta \Sigma_i^d = \text{Diag}(\Delta \sigma_{i1}, \dots, \Delta \sigma_{id}), \quad (11)$$

so that

$$\tilde{\Sigma}_i^d = \text{Diag}(\sigma_{i1} + \Delta \sigma_{i1}, \dots, \sigma_{id} + \Delta \sigma_{id})$$

with $\sigma_{ij} + \Delta \sigma_{ij} > 0$.

4.1. Initialization-Error Mismatch $\mathcal{E}_{\text{init}}^d$

We begin by noting that

$$\rho_0^d(x) = \sum_{i \in I} w_i \varphi_{i,0}^d(x), \quad \tilde{\rho}_0^d(x) = \sum_{i \in I} \tilde{w}_i \tilde{\varphi}_{i,0}^d(x),$$

where $\varphi_{i,0}^d$ and $\tilde{\varphi}_{i,0}^d$ are the Gaussian densities

$$\varphi_{i,t}^d := \mathcal{N}(m_i^d, \Sigma_i^d + \kappa_t C^d), \quad \tilde{\varphi}_{i,t}^d := \mathcal{N}(\tilde{m}_i^d, \tilde{\Sigma}_i^d + \kappa_t C^d),$$

with $\kappa_t := (T-t)/T$, evaluated at $t=0$. Thus, the initialization error in Proposition 4.1 reduces to the discrepancy between two Gaussian mixtures with misspecified weights, means and covariances. We quantify this mismatch in the following proposition.

Proposition 4.3. *We have the upper bound*

$$\mathcal{E}_{\text{init}}^d \leq \text{KL}(w \parallel \tilde{w}) + \sum_{i \in I} w_i \text{KL}(\varphi_{i,0}^d \parallel \tilde{\varphi}_{i,0}^d), \quad (12)$$

where

$$\text{KL}(w \parallel \tilde{w}) = \sum_{i \in I} w_i \log\left(\frac{w_i}{\tilde{w}_i}\right). \quad (13)$$

Moreover, combining Assumption 4.2 with (11) yields the explicit expression

$$\begin{aligned} \text{KL}(\varphi_{i,0}^d \parallel \tilde{\varphi}_{i,0}^d) &= \frac{1}{2} \sum_{j=1}^d \left[\frac{(\Delta m_{ij})^2}{\sigma_{ij} + \Delta \sigma_{ij} + \lambda_j} \right. \\ &\quad \left. + \log\left(1 + \frac{\Delta \sigma_{ij}}{\sigma_{ij} + \lambda_j}\right) - \frac{\Delta \sigma_{ij}}{\sigma_{ij} + \Delta \sigma_{ij} + \lambda_j} \right]. \end{aligned} \quad (14)$$

The bound (12) naturally splits into a weight-mismatch term (13) and a within-component Gaussian mismatch term (14):

- The weight term can be controlled, for example, by assuming $\tilde{w}_i = w_i(1 + \eta_i)$, with $\eta_i \in (-\eta, \eta)$ for some $\eta \in (0, 1)$.
- Controlling (14) uniformly in d instead amounts to ensuring that the coordinatewise contributions are summable as $d \rightarrow \infty$. For example, using $\log(1+r) \leq r$ for $r > -1$, one obtains the sufficient conditions

$$\begin{aligned} \sup_{i \in I} \sum_{j \geq 1} \frac{(\Delta m_{ij})^2}{\sigma_{ij} + \Delta \sigma_{ij} + \lambda_j} &< \infty, \\ \sup_{i \in I} \sum_{j \geq 1} \frac{(\Delta \sigma_{ij})^2}{(\sigma_{ij} + \lambda_j)(\sigma_{ij} + \Delta \sigma_{ij} + \lambda_j)} &< \infty. \end{aligned} \quad (15)$$

4.2. Score-Error Mismatch $\mathcal{E}_{\text{score},T}^d$

We now turn to the score-error contribution, quantified by the Γ^d -weighted energy

$$\mathcal{E}_{\text{score},T}^d := \int_0^T \mathbb{E}_{\rho_t^d} \|(\Gamma^d)^{1/2} \epsilon_t^d(X)\|^2 dt. \quad (16)$$

In the Gaussian-mixture setting, the discrepancy ϵ_t^d admits the decomposition

$$\begin{aligned} \epsilon_t^d(x) &= \sum_{i \in I} p_{i,t}(x) (\tilde{S}_{i,t}^d(x) - S_{i,t}^d(x)) \\ &\quad + \sum_{i \in I} (\tilde{p}_{i,t}(x) - p_{i,t}(x)) \tilde{S}_{i,t}^d(x), \end{aligned} \quad (17)$$

where $p_{i,t}(x) = \frac{w_i \varphi_{i,t}^d(x)}{\rho_t^d(x)}$ and $\tilde{p}_{i,t}(x) = \frac{\tilde{w}_i \tilde{\varphi}_{i,t}^d(x)}{\tilde{\rho}_t^d(x)}$ are the exact and perturbed responsibilities, and

$$\begin{aligned} S_{i,t}^d(x) &:= -\left(\Sigma_i^d + \kappa_t C^d\right)^{-1} (x - m_i^d), \\ \tilde{S}_{i,t}^d(x) &:= -\left(\tilde{\Sigma}_i^d + \kappa_t C^d\right)^{-1} (x - \tilde{m}_i^d). \end{aligned}$$

We bound the two contributions in (17) in the following proposition.

Proposition 4.4. *For each $t \in [0, T]$, we have*

$$\mathbb{E}_{\rho_t^d} \left\| \sum_{i \in I} p_{i,t}(X) (\Gamma^d)^{1/2} (\tilde{S}_{i,t}^d - S_{i,t}^d)(X) \right\|^2 \leq B_{\text{comp}}^d(t), \quad (18)$$

with

$$B_{\text{comp}}^d(t) := 2 \sum_{i \in I} w_i \sum_{j=1}^d \gamma_j \frac{(\Delta m_{ij})^2 + \frac{(\Delta \sigma_{ij})^2}{\sigma_{ij} + \kappa_t \lambda_j}}{(\sigma_{ij} + \Delta \sigma_{ij} + \kappa_t \lambda_j)^2}.$$

Moreover, there exists an explicit function $B_{\text{resp}}^d(t)$ (given in Appendix B.3) such that

$$\mathbb{E}_{\rho_t^d} \left\| \sum_{i \in I} (\tilde{p}_{i,t} - p_{i,t})(X) (\Gamma^d)^{1/2} \tilde{S}_{i,t}^d(X) \right\|^2 \leq B_{\text{resp}}^d(t). \quad (19)$$

Consequently,

$$\mathcal{E}_{\text{score},T}^d \leq \int_0^T (B_{\text{comp}}^d(t) + B_{\text{resp}}^d(t)) dt. \quad (20)$$

Appendix B.4 states the full set of assumptions on Δw_i , Δm_{ij} , and $\Delta \sigma_{ij}$ ensuring that the bounds (18) and (19) remain uniform as $d \rightarrow \infty$; here we highlight a few key points, with particular emphasis on the role of the preconditioner spectrum (γ_j) :

- The term $B_{\text{comp}}^d(t)$ depends on $(\Delta m_{ij}, \Delta \sigma_{ij})$ only through γ_j -weighted coordinatewise contributions. Accordingly, a sufficient condition for dimension-uniform control is to require that the corresponding series are summable

$$\sup_{i \in I} \sum_{j \geq 1} \gamma_j \frac{(\Delta m_{ij})^2}{(\sigma_{ij} + \Delta \sigma_{ij})^2} < \infty,$$

$$\sup_{i \in I} \sum_{j \geq 1} \gamma_j \frac{(\Delta \sigma_{ij})^2}{\sigma_{ij} (\sigma_{ij} + \Delta \sigma_{ij})^2} < \infty.$$

- The term $B_{\text{resp}}^d(t)$ is more delicate because it couples weight perturbations and component perturbations through the Gaussian-mixture responsibilities. Its full control is technical and is deferred to Appendix B.4. Here we only give a glimpse of the mechanism by which component perturbations enter via the responsibilities, and isolate a few representative conditions under which this effect can be bounded in terms of (i) a density-ratio factor $\mathbb{E}_{\tilde{\rho}_t^d}[(\rho_t^d / \tilde{\rho}_t^d)^2(X)]$ and (ii) a collection of γ_j -weighted series. In the ideal case $\Delta m_{ij} = 0$ (perfect mean match), these conditions reduce to

$$\sup_{i \in I} \sum_{j \geq 1} \frac{\gamma_j^p}{(\sigma_{ij} + \Delta \sigma_{ij})^p} < \infty, \text{ for } p = 1, 2,$$

together with uniform control of the variance ratio $(\sigma_{ij} + \Delta \sigma_{ij}) / \sigma_{ij}$. When the means are misspecified, additional weighted summability conditions are required:

$$\sup_{i \in I} \sum_{j \geq 1} \gamma_j^p \frac{(\Delta m_{ij})^2}{(\sigma_{ij} + \Delta \sigma_{ij})^{1+p}} < \infty, \text{ for } p = 1, 2,$$

and

$$\sup_{i \in I} \sum_{j \geq 1} \gamma_j^2 \frac{(\Delta m_{ij})^4}{(\sigma_{ij} + \Delta \sigma_{ij})^4} < \infty.$$

These conditions highlight the importance of preconditioning for designing ALD algorithms that remain robust in high dimensions: while Theorem 3.1 allows choices such as $\gamma_j = \lambda_j$ (or even $\gamma_j = 1$), provided λ_j decays sufficiently fast relative to σ_{ij} , in the presence of score errors it becomes crucial to choose (γ_j) with sufficient decay to prevent the error terms from accumulating across coordinates and destroying dimension-uniform control.

5. Numerical Experiments

We conclude the analysis by presenting simple numerical experiments that corroborate our theoretical findings: for targets given by truncations of an infinite-dimensional Gaussian-mixture law, multimodal sampling via preconditioned ALD can be made dimension-robust. We estimate the empirical KL divergence between the truncated target ρ_{\star}^d and the ALD output law $\rho_T^{\text{ALD},d}$ as the dimension increases, and we compare the regimes discussed throughout the paper. Our goal is twofold: to highlight the impact of design choices that are intrinsic to the infinite-dimensional setting, and to illustrate the role of the preconditioner in ensuring stability under score error. Implementation and further details are provided in Appendix D.

5.1. Annealing-Induced Bias vs. Dimension

We consider a two-component infinite-dimensional Gaussian-mixture target with weights $(0.75, 0.25)$, separated means $m_2 - m_1 = 10 e_1$, and covariances $\Sigma_1 = \tau_1 \Sigma$ and $\Sigma_2 = \tau_2 \Sigma$, where $\tau_1 = 1.2$, $\tau_2 = 2$, and $\Sigma = \text{Diag}(j^{-1.25})_{j \geq 1}$. We study its truncations ρ_{\star}^d at dimensions $d \in \{1, 5, \dots, 65\}$. We work in the idealized setting of Section 3, with the exact score along the annealing path and with initial samples drawn from the smoothed initialization $\rho_0^d = \rho_{\star}^d * \mathcal{N}(0, C^d)$. We fix a common time horizon T and we run ALD for each truncation dimension d , and report the empirical bias $\text{KL}(\rho_{\star}^d \| \rho_T^{\text{ALD},d})$.

Within this controlled setting, we compare two regimes. In the first, we follow (8) and run ALD with diagonal preconditioner $\Gamma = \text{Diag}(j^{-1.5})_{j \geq 1}$ and smoothing $C = \text{Diag}(40 \cdot j^{-2.7})_{j \geq 1}$ (the factor 40 sets the overall smooth-

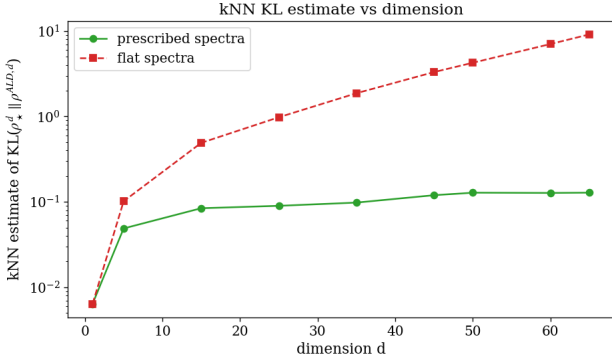


Figure 3. Annealed-induced bias across dimensions. Empirical $\text{KL}(\rho_*^d \parallel \rho^{\text{ALD},d})$ as a function of the truncation dimension d , shown on a logarithmic y -axis. The green curve corresponds to the prescribed spectra $\Gamma = \text{Diag}(j^{-1.5})_{j \geq 1}$ and $C = \text{Diag}(40 \cdot j^{-2.7})_{j \geq 1}$, while the red curve corresponds to the flat-spectrum choice $\Gamma = I$ and $C = 40I$. The KL is estimated via k NN with $k = 20$; robustness to k is reported in Appendix D.

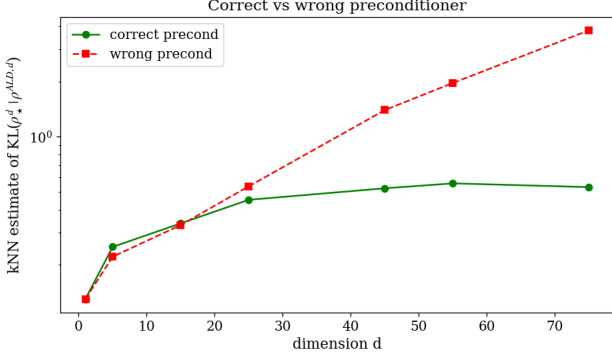


Figure 4. Preconditioning and dimension dependence of the KL. Empirical $\text{KL}(\rho_*^d \parallel \rho^{\text{ALD},d})$ as a function of the truncation dimension d , shown on a logarithmic y -axis. The green curve corresponds to runs of the ALD sampler with preconditioner $\Gamma = \text{Diag}(j^{-3.5})_{j \geq 1}$, while the red curve corresponds to runs with $\Gamma = \text{Diag}(j^{-1})_{j \geq 1}$. The KL is estimated via k NN with $k = 20$; robustness to k is reported in Appendix D.

ing scale). In the second, the target ρ_*^d is unchanged but we use the identity preconditioner and a flat-spectrum smoothing, i.e. $\Gamma = I$ and $C = 40I$. Figure 3 contrasts the two behaviors on a logarithmic scale: under the prescribed spectra the empirical $\text{KL}(\rho_*^d \parallel \rho^{\text{ALD},d})$ stays uniformly small as d increases, whereas under the flat-spectrum choice it grows rapidly with d . This illustrates that (8) reflects a genuine high-dimensional stability constraint rather than a proof artefact.

5.2. The Importance of Preconditioning

We now introduce error in both the initialization and the score. To isolate the role in achieving dimension-uniformity that our theory attributes to the preconditioner, we initialize

the ALD diffusion from a mixture with incorrect weights $(0.1, 0.9)$ but with the same component means and covariances as the target, so that the initialization error does not play a role in the stability analysis (the second sum on the right-hand side of (12) is zero). The ALD drift, in contrast, is computed under a misspecified mixture in which the component covariances are perturbed.

Specifically, in Figure 4 we consider an infinite-dimensional bimodal Gaussian mixture target with weights $(0.75, 0.25)$, identical covariances $\Sigma_1 = \Sigma_2 = \text{Diag}(j^{-2})_{j \geq 1}$, and separated means $m_2 - m_1 = 10e_1$. We study truncations at dimensions $d \in \{1, 5, \dots, 75\}$. Following Section 4.2 and the conditions of Appendix B.4, we introduce a covariance perturbation $\Delta\sigma_{ij}$ whose spectrum decays as $(j^{-3.5})_{j \geq 1}$. We then compare two preconditioners: one that satisfies the conditions of Appendix B.4, $\Gamma = \text{Diag}(j^{-3.5})_{j \geq 1}$, and one that violates them, $\Gamma = \text{Diag}(j^{-1})_{j \geq 1}$. The contrast is once again evident: with the admissible preconditioner the error remains uniformly controlled as d grows, whereas with the non-admissible one it increases with dimension—highlighting that, under score error, *preconditioning is crucial for dimension-robust stability*.

6. Discussion and Future Work

We studied the robustness of continuous-time annealed Langevin dynamics with respect to dimension in a multimodal setting. We showed that, within a well-defined infinite-dimensional framework, appropriate design choices yield dimension-uniform behavior, improving upon recent bounds that degrade with dimension. Our analysis highlights the central role of preconditioning—a message that is not surprising, and that connects our work to recent function-space diffusion models literature (Pidstrigach et al., 2024; Baldassari et al., 2025). We derive explicit dimension-dependent error bounds and identify conditions under which they remain uniform, clarifying the interplay between the mixture component means and covariances, the annealing smoothing, and the preconditioner. As the authors of (Baldassari et al., 2023; Pidstrigach et al., 2024; Baldassari et al., 2025), we adopt simplifying assumptions, notably that the mixture covariances are co-diagonalizable; this restriction is less limiting here, since we allow infinitely many mixture components, which still permit the approximation of rich distributions. Several questions remain open, including posterior sampling in Bayesian nonlinear inverse problems, where classical Langevin is known to struggle (Bohr & Nickl, 2024; Nickl, 2023). Developing an ALD analogue of the theory in Baldassari et al. (2025) in this setting is a natural next step, and one we are actively pursuing.

Impact Statement

This paper presents work whose goal is to advance the field of machine learning. There are many potential societal consequences of our work, none of which we feel must be specifically highlighted here.

References

Albergo, M., Boffi, N. M., and Vanden-Eijnden, E. Stochastic interpolants: A unifying framework for flows and diffusions. *Journal of Machine Learning Research*, 26(209):1–80, 2025.

Astolfi, P., Careil, M., Hall, M., Manas, O., Muckley, M., Verbeek, J., Soriano, A., and Drozdzal, M. Consistency-diversity-realism Pareto fronts of conditional image generative models. *arXiv:2406.10429*, 2024.

Baldassari, L., Siahkoohi, A., Garnier, J., Solna, K., and de Hoop, M. V. Conditional score-based diffusion models for Bayesian inference in infinite dimensions. *Advances in Neural Information Processing Systems*, 36:24262–24290, 2023.

Baldassari, L., Siahkoohi, A., Garnier, J., Solna, K., and de Hoop, M. V. Taming score-based diffusion priors for infinite-dimensional nonlinear inverse problems. *arXiv preprint arXiv:2405.15676*, 2024.

Baldassari, L., Garnier, J., Solna, K., and de Hoop, M. V. Preconditioned Langevin dynamics with score-based generative models for infinite-dimensional linear Bayesian inverse problems. *arXiv preprint arXiv:2505.18276*, 2025.

Bandeira, A. S., Maillard, A., Nickl, R., and Wang, S. On free energy barriers in Gaussian priors and failure of cold start MCMC for high-dimensional unimodal distributions. *Philosophical Transactions of the Royal Society A*, 381(2247):20220150, 2023.

Beskos, A., Girolami, M., Lan, S., Farrell, P. E., and Stuart, A. M. Geometric mcmc for infinite-dimensional inverse problems. *Journal of Computational Physics*, 335:327–351, 2017.

Block, A., Mroueh, Y., and Raklin, A. Generative modeling with denoising auto-encoders and Langevin sampling. *arXiv preprint arXiv:2002.00107*, 2020.

Bohr, J. and Nickl, R. On log-concave approximations of high-dimensional posterior measures and stability properties in non-linear inverse problems. *Ann. Inst. H. Poincaré Probab. Statist.*, 60:2619–2667, 2024.

Bond-Taylor, S. and Willcocks, C. G. ∞ -diff: Infinite resolution diffusion with subsampled mollified states. *International Conference on Learning Representations*, 2024.

Bradley, A. and Nakkiran, P. Classifier-free guidance is a predictor-corrector. *arXiv:2408.09000*, 2024.

Cattiaux, P., Cordero-Encinar, P., and Guillin, A. Diffusion annealed Langevin dynamics: a theoretical study. *arXiv preprint arXiv:2511.10406*, 2025.

Chewi, S., Erdogdu, M. A., Li, M., Shen, R., and Zhang, M. S. Analysis of Langevin Monte Carlo from Poincaré to log-Sobolev. *Foundations of Computational Mathematics*, 25(4):1345–1395, 2025.

Cordero-Encinar, P., Akyildiz, O. D., and Duncan, A. B. Non-asymptotic analysis of diffusion annealed Langevin Monte Carlo for generative modelling. *arXiv preprint arXiv:2502.09306*, 2025.

Cotter, S. L., Roberts, G. O., Stuart, A. M., and White, D. MCMC methods for functions: modifying old algorithms to make them faster. *Statistical Science*, pp. 424–446, 2013.

Cui, T., Law, K. J., and Marzouk, Y. M. Dimension-independent likelihood-informed MCMC. *Journal of Computational Physics*, 304:109–137, 2016.

Dalalyan, A. S. Theoretical guarantees for approximate sampling from smooth and log-concave densities. *Journal of the Royal Statistical Society Series B: Statistical Methodology*, 79(3):651–676, 2017.

Dong, J. and Tong, X. T. Spectral gap of replica exchange Langevin diffusion on mixture distributions. *Stochastic Processes and their Applications*, 151:451–489, 2022.

Durmus, A., Roberts, G. O., Vilmart, G., and Zygalakis, K. C. Fast Langevin based algorithm for MCMC in high dimensions. *The Annals of Applied Probability*, 27:2195–2237, 2017.

Durmus, A., Majewski, S., and Miasojedow, B. Analysis of Langevin Monte Carlo via convex optimization. *Journal of Machine Learning Research*, 20(73):1–46, 2019.

Franzese, G. and Michiardi, P. Generative diffusion models in infinite dimensions: a survey. *Philosophical Transactions A*, 383(2299):20240322, 2025.

Franzese, G., Corallo, G., Rossi, S., Heinonen, M., Filippone, M., and Michiardi, P. Continuous-time functional diffusion processes. *Advances in Neural Information Processing Systems*, 36:37370–37400, 2023.

Gelfand, S. B. and Mitter, S. K. On sampling methods and annealing algorithms. Technical report, 1990.

Guo, W., Tao, M., and Chen, Y. Provable benefit of annealed Langevin Monte Carlo for non-log-concave sampling. *International Conference on Learning Representations*, 2025.

Hagemann, P., Mildnerger, S., Ruthotto, L., Steidl, G., and Yang, N. T. Multilevel diffusion: Infinite dimensional score-based diffusion models for image generation. *SIAM Journal on Mathematics of Data Science*, 7(3):1337–1366, 2025.

Hairer, M. An introduction to stochastic PDEs. *arXiv preprint arXiv:0907.4178*, 2009.

Hairer, M., Stuart, A. M., and Vollmer, S. J. Spectral gaps for a Metropolis–Hastings algorithm in infinite dimensions. *The Annals of Applied Probability*, 24:2455–2490, 2014.

Ho, J. and Salimans, T. Classifier-free diffusion guidance. *arXiv:2207.12598*, 2022.

Kerrigan, G., Ley, J., and Smyth, P. Diffusion generative models in infinite dimensions. *International Conference on Artificial Intelligence and Statistics*, 2023.

Kirkpatrick, S., Gelatt Jr, C. D., and Vecchi, M. P. Optimization by simulated annealing. *Science*, 220(4598):671–680, 1983.

Lim, J. H., Kovachki, N. B., Baptista, R., Beckham, C., Azizzadenesheli, K., Kossaifi, J., Voleti, V., Song, J., Kreis, K., Kautz, J., et al. Score-based diffusion models in function space. *Journal of Machine Learning Research*, 26(158):1–62, 2025.

Ma, Y.-A., Chen, Y., Jin, C., Flammarion, N., and Jordan, M. I. Sampling can be faster than optimization. *Proceedings of the National Academy of Sciences*, 116(42):20881–20885, 2019.

McLachlan, G. J. and Peel, D. *Finite mixture models*. John Wiley & Sons, 2000.

Neal, R. M. Annealed importance sampling. *Statistics and Computing*, 11(2):125–139, 2001.

Nickl, R. *Bayesian non-linear statistical inverse problems*. EMS press Berlin, 2023.

Parisi, G. Correlation functions and computer simulations. *Nuclear Physics B*, 180(3):378–384, 1981.

Pavasovic, K., Verbeek, J., Birulio, G., and Mezard, M. Classifier-free guidance: From high-dimensional analysis to generalized guidance forms. *arXiv:2502.07849v2*, 2025.

Pérez-Cruz, F. Kullback-Leibler divergence estimation of continuous distributions. In *2008 IEEE international symposium on information theory*, pp. 1666–1670. IEEE, 2008.

Pidstrigach, J., Marzouk, Y., Reich, S., and Wang, S. Infinite-dimensional diffusion models. *Journal of Machine Learning Research*, 25(414):1–52, 2024.

Roberts, G. O. and Rosenthal, J. S. Optimal scaling of discrete approximations to Langevin diffusions. *Journal of the Royal Statistical Society: Series B (Statistical Methodology)*, 60(1):255–268, 1998.

Roberts, G. O. and Tweedie, R. L. Exponential convergence of Langevin distributions and their discrete approximations. *Bernoulli*, 2:341–363, 1996.

Schlichting, A. Poincaré and log-sobolev inequalities for mixtures. *Entropy*, 21(1):89, 2019.

Song, Y. and Ermon, S. Generative modeling by estimating gradients of the data distribution. *Advances in Neural Information Processing Systems*, 32, 2019.

Song, Y. and Ermon, S. Improved techniques for training score-based generative models. *Advances in Neural Information Processing Systems*, 33:12438–12448, 2020.

Song, Y., Sohl-Dickstein, J., Kingma, D. P., Kumar, A., Ermon, S., and Poole, B. Score-based generative modeling through stochastic differential equations. *International Conference on Learning Representations*, 2021.

Sun, Y., Wu, Z., Chen, Y., Feng, B. T., and Bouman, K. L. Provable probabilistic imaging using score-based generative priors. *IEEE Transactions on Computational Imaging*, 10:1290–1305, 2024.

Vempala, S. and Wibisono, A. Rapid convergence of the unadjusted Langevin algorithm: Isoperimetry suffices. *Advances in Neural Information Processing Systems*, 32, 2019.

Wang, Q., Kulkarni, S. R., and Verdú, S. Divergence estimation for multidimensional densities via k -nearest-neighbor distances. *IEEE Transactions on Information Theory*, 55(5):2392–2405, 2009.

Wang, X., Dufour, N., Andreou, N., Cani, M., Abrevaya, V., Picard, D., and Kalogeiton, V. Analysis of classifier-free guidance weight schedulers. *Transactions on Machine Learning Research*, 2024. ISSN 2835-8856.

Wu, Y., Chen, M., Li, Z., Wang, M., and Wei, Y. Theoretical insights for diffusion guidance: A case study for Gaussian mixture models. *International Conference on Machine Learning*, 2024.

Yehezkel, S., Dahary, O., Voynov, A., and Cohen-Or, D. Navigating with annealing guidance scale in diffusion space. In *Proceedings of the SIGGRAPH Asia 2025 Conference Papers*, pp. 1–11, 2025.

Zilberstein, N., Dick, C., Doost-Mohammady, R., Sabharwal, A., and Segarra, S. Annealed Langevin dynamics for massive MIMO detection. *IEEE Transactions on Wireless Communications*, 22(6):3762–3776, 2022.

A. Proofs of Section 3

Before proving Theorem 3.1, we recall a standard lemma. For completeness, we include the proof below.

Lemma A.1. *Let*

$$\begin{cases} dX_t^d = a_t(X_t^d) dt + \sqrt{2\Gamma^d} dW_t^d, & X_0^d \sim \mu^d, \\ dY_t^d = b_t(Y_t^d) dt + \sqrt{2\Gamma^d} dW_t^d, & Y_0^d \sim \nu^d, \end{cases}$$

and denote by P_{X^d} and P_{Y^d} the path laws of $(X_t^d)_{t \in [0, T]}$ and $(Y_t^d)_{t \in [0, T]}$. Then

$$\text{KL}(P_{X^d} \parallel P_{Y^d}) = \text{KL}(\mu^d \parallel \nu^d) + \frac{1}{4} \mathbb{E}_{X^d \sim P_{X^d}} \int_0^T \|a_t(X_t^d) - b_t(X_t^d)\|_{(\Gamma^d)^{-1}}^2 dt,$$

where $\|u\|_{(\Gamma^d)^{-1}}^2 := \langle u, (\Gamma^d)^{-1} u \rangle$.

Proof. In dimension d , Girsanov formula gives

$$\begin{aligned} \frac{dP_{X^d}}{dP_{Y^d}} = \frac{\mu^d(X_0^d)}{\nu^d(X_0^d)} \exp \left\{ \int_0^T \left\langle (2\Gamma^d)^{-1}(a_t(X_t^d) - b_t(X_t^d)), dX_t^d \right\rangle \right. \\ \left. - \frac{1}{2} \int_0^T \left(\|(2\Gamma^d)^{-1/2}a_t(X_t^d)\|^2 - \|(2\Gamma^d)^{-1/2}b_t(X_t^d)\|^2 \right) dt \right\}. \end{aligned}$$

Taking the logarithm yields

$$\begin{aligned} \log \frac{dP_{X^d}}{dP_{Y^d}} = \log \frac{\mu^d(X_0^d)}{\nu^d(X_0^d)} + \int_0^T \left\langle (2\Gamma^d)^{-1}(a_t(X_t^d) - b_t(X_t^d)), dX_t^d \right\rangle \\ - \frac{1}{2} \int_0^T \left(\|(2\Gamma^d)^{-1/2}a_t(X_t^d)\|^2 - \|(2\Gamma^d)^{-1/2}b_t(X_t^d)\|^2 \right) dt. \end{aligned}$$

Using the SDE for dX_t^d , we have

$$\begin{aligned} \left\langle (2\Gamma^d)^{-1}(a_t - b_t)(X_t^d), dX_t^d \right\rangle = \left\langle (2\Gamma^d)^{-1/2}(a_t - b_t)(X_t^d), (2\Gamma^d)^{-1/2}a_t(X_t^d) \right\rangle dt \\ + \left\langle (2\Gamma^d)^{-1/2}(a_t - b_t)(X_t^d), dW_t^d \right\rangle. \end{aligned}$$

The stochastic integral has mean zero under P_{X^d} . Since $\text{KL}(P_{X^d} \parallel P_{Y^d}) = \mathbb{E}_{P_{X^d}} \left[\log \frac{dP_{X^d}}{dP_{Y^d}} \right]$, taking expectations gives

$$\begin{aligned} \text{KL}(P_{X^d} \parallel P_{Y^d}) = \text{KL}(\mu^d \parallel \nu^d) + \mathbb{E}_{P_{X^d}} \int_0^T \left\langle (2\Gamma^d)^{-1/2}(a_t - b_t)(X_t^d), (2\Gamma^d)^{-1/2}a_t(X_t^d) \right\rangle dt \\ - \frac{1}{2} \mathbb{E}_{P_{X^d}} \int_0^T \left(\|(2\Gamma^d)^{-1/2}a_t(X_t^d)\|^2 - \|(2\Gamma^d)^{-1/2}b_t(X_t^d)\|^2 \right) dt. \end{aligned}$$

By the identity

$$\langle u - v, u \rangle - \frac{1}{2} (\|u\|^2 - \|v\|^2) = \frac{1}{2} \|u - v\|^2,$$

applied to $u = (2\Gamma^d)^{-1/2}a_t(X_t^d)$ and $v = (2\Gamma^d)^{-1/2}b_t(X_t^d)$, we obtain

$$\text{KL}(P_{X^d} \parallel P_{Y^d}) = \text{KL}(\mu^d \parallel \nu^d) + \frac{1}{4} \mathbb{E}_{P_{X^d}} \int_0^T \|(2\Gamma^d)^{-1/2}(a_t - b_t)(X_t^d)\|^2 dt.$$

□

We are now ready to prove Theorem 3.1. The proof builds on ideas from Appendix A of (Guo et al., 2025), adapted to our infinite-dimensional setting.

A.1. Proof of Theorem 3.1

Let \mathbb{Q}^d be the path measure on $C([0, T^d]; \mathbb{R}^d)$ of the ALD diffusion (4) initialized at $X_0^d \sim \rho_0^d$, and let $\pi_{T^d}(\omega) = \omega(T^d)$ be the evaluation map. For any path measure \mathbb{P} on $C([0, T^d]; \mathbb{R}^d)$, the data-processing inequality yields

$$\text{KL}((\pi_{T^d})_\# \mathbb{P} \parallel (\pi_{T^d})_\# \mathbb{Q}^d) \leq \text{KL}(\mathbb{P} \parallel \mathbb{Q}^d).$$

We apply this with a reference path measure $\mathbb{P}^{v,d}$ constructed as follows. Let $\mathbb{P}^{v,d}$ denote the path law of

$$dX_t^d = \Gamma^d (\nabla \log \rho_t^d + v_t^d) (X_t^d) dt + \sqrt{2\Gamma^d} dW_t^d, \quad X_0^d \sim \rho_0^d, \quad (21)$$

where the annealing path is

$$\rho_t^d = \rho_\star^d * \mathcal{N}\left(0, \frac{T^d - t}{T^d} C^d\right), \quad t \in [0, T^d].$$

We choose $v^d = (v_t^d)_{t \in [0, T^d]}$ so that $\text{Law}_{\mathbb{P}^{v,d}}(X_t^d) = \rho_t^d$ for all $t \in [0, T^d]$. Since the diffusion matrix is constant ($2\Gamma^d$), the corresponding Fokker–Planck equation reduces to

$$\partial_t \rho_t^d = -\nabla \cdot (\rho_t^d \Gamma^d v_t^d). \quad (22)$$

On the other hand, the Gaussian-smoothing path satisfies the backward heat equation

$$\partial_t \rho_t^d = -\frac{1}{2T^d} \nabla \cdot (C^d \nabla \rho_t^d), \quad (23)$$

because differentiating with respect to the covariance parameter introduces a factor $1/2$, and $\frac{d}{dt} \left(\frac{T^d - t}{T^d} \right) = -\frac{1}{T^d}$. Comparing (22) and (23), an admissible choice is

$$\Gamma^d v_t^d = \frac{1}{2T^d} C^d \nabla \log \rho_t^d, \quad \text{i.e.} \quad v_t^d = \frac{1}{2T^d} (\Gamma^d)^{-1} C^d \nabla \log \rho_t^d. \quad (24)$$

With this choice, $(\pi_{T^d})_\# \mathbb{P}^{v,d} = \rho_{T^d}^d = \rho_\star^d$. Since $(\pi_{T^d})_\# \mathbb{Q}^d = \rho_{T^d}^{\text{ALD},d}$ by definition, we have

$$\text{KL}(\rho_\star^d \parallel \rho_{T^d}^{\text{ALD},d}) \leq \text{KL}(\mathbb{P}^{v,d} \parallel \mathbb{Q}^d). \quad (25)$$

It therefore remains to obtain an explicit upper bound on the path-space divergence $\text{KL}(\mathbb{P}^{v,d} \parallel \mathbb{Q}^d)$.

By Lemma A.1, we have

$$\begin{aligned} \text{KL}(\mathbb{P}^{v,d} \parallel \mathbb{Q}^d) &= \frac{1}{4} \mathbb{E}_{\mathbb{P}^{v,d}} \int_0^{T^d} \|\Gamma^d v_t^d(X_t^d)\|_{(\Gamma^d)^{-1}}^2 dt = \frac{1}{4} \int_0^{T^d} \int \langle v_t^d, \Gamma^d v_t^d \rangle d\rho_t^d dt \\ &= \frac{1}{16(T^d)^2} \int_0^{T^d} \int \langle \nabla \log \rho_t^d, A^d \nabla \log \rho_t^d \rangle d\rho_t^d dt, \end{aligned} \quad (26)$$

where $A^d := C^d (\Gamma^d)^{-1} C^d$.

Fix $t \in [0, T^d]$. Since ρ_t^d is a Gaussian mixture,

$$\rho_t^d = \sum_{i \in I} w_i \mathcal{N}\left(m_i^d, \Sigma_i^d + \frac{T^d - t}{T^d} C^d\right), \quad \rho_t^d(x) = \sum_{i \in I} w_i \varphi_{i,t}(x),$$

and with responsibilities $p_{i,t}(x) := \frac{w_i \varphi_{i,t}(x)}{\rho_t^d(x)}$ we obtain

$$\nabla \log \rho_t^d(x) = - \sum_{i \in I} p_{i,t}(x) \left(\Sigma_i^d + \frac{T^d - t}{T^d} C^d \right)^{-1} (x - m_i^d).$$

Since $z \mapsto z^\top A^d z$ is convex ($A^d \succeq 0$), Jensen's inequality yields

$$\langle \nabla \log \rho_t^d(x), A^d \nabla \log \rho_t^d(x) \rangle \leq \sum_{i \in I} p_{i,t}(x) (x - m_i^d)^\top \left(\Sigma_i^d + \frac{T^d - t}{T^d} C^d \right)^{-1} A^d \left(\Sigma_i^d + \frac{T^d - t}{T^d} C^d \right)^{-1} (x - m_i^d).$$

Integrating against $\rho_t^d(x) dx$ and using $\rho_t^d p_{i,t} = w_i \varphi_{i,t}$ gives

$$\int \langle \nabla \log \rho_t^d, A^d \nabla \log \rho_t^d \rangle d\rho_t^d \leq \sum_{i \in I} w_i \text{Tr} \left(A^d \left(\Sigma_i^d + \frac{T^d - t}{T^d} C^d \right)^{-1} \right),$$

where we used that, in the diagonal setting, all matrices commute and $\text{Cov}(\varphi_{i,t}) = \Sigma_i^d + \frac{T^d - t}{T^d} C^d$. Plugging this into (26) yields

$$\text{KL}(\mathbb{P}^{v,d} \| \mathbb{Q}^d) \leq \frac{1}{16(T^d)^2} \sum_{i \in I} w_i \int_0^{T^d} \text{Tr} \left(A^d \left(\Sigma_i^d + \frac{T^d - t}{T^d} C^d \right)^{-1} \right) dt.$$

Changing variables $s := \frac{T^d - t}{T^d} \in [0, 1]$ (so $dt = -T^d ds$) gives

$$\int_0^{T^d} \text{Tr} \left(A^d \left(\Sigma_i^d + \frac{T^d - t}{T^d} C^d \right)^{-1} \right) dt = T^d \int_0^1 \text{Tr} \left(A^d (\Sigma_i^d + sC^d)^{-1} \right) ds.$$

Since A^d , C^d , and Σ_i^d are diagonal with eigenvalues λ_j^2/γ_j , λ_j , and σ_{ij} , respectively, we have

$$\text{Tr} \left(A^d (\Sigma_i^d + sC^d)^{-1} \right) = \sum_{j=1}^d \frac{\lambda_j^2}{\gamma_j(\sigma_{ij} + s\lambda_j)}.$$

Therefore,

$$\text{KL}(\mathbb{P}^{v,d} \| \mathbb{Q}^d) \leq \frac{1}{16T^d} \sum_{i \in I} w_i \sum_{j=1}^d \frac{\lambda_j^2}{\gamma_j} \int_0^1 \frac{ds}{\sigma_{ij} + s\lambda_j} = \frac{1}{16T^d} \sum_{i \in I} w_i \sum_{j=1}^d \frac{\lambda_j}{\gamma_j} \log \left(1 + \frac{\lambda_j}{\sigma_{ij}} \right).$$

Finally, combining this estimate with (25) finally gives the desired bound

$$\text{KL}(\rho_\star^d \| \rho_{T^d}^{\text{ALD},d}) \leq \frac{1}{16T^d} \sum_{i \in I} w_i \sum_{j=1}^d \frac{\lambda_j}{\gamma_j} \log \left(1 + \frac{\lambda_j}{\sigma_{ij}} \right).$$

Now fix $\epsilon > 0$. Choosing

$$T^d = \frac{1}{16\epsilon} \sum_{i \in I} w_i \sum_{j=1}^d \frac{\lambda_j}{\gamma_j} \log \left(1 + \frac{\lambda_j}{\sigma_{ij}} \right)$$

yields

$$\text{KL}(\rho_\star^d \| \rho_{T^d}^{\text{ALD},d}) \leq \epsilon.$$

B. Proofs of Section 4

B.1. Proof of Proposition 4.1

As in Subsection A.1, we consider the reference SDE

$$dX_t^d = \Gamma^d (\nabla \log \rho_t^d + v_t^d) (X_t^d) dt + \sqrt{2\Gamma^d} dW_t^d, \quad X_0^d \sim \rho_0^d,$$

with path measure $\mathbb{P}^{v,d}$ and $v^d = (v_t^d)_{t \in [0, T^d]}$ so that $\text{Law}_{\mathbb{P}^{v,d}}(X_t^d) = \rho_t^d$, and compare it to the approximate SDE

$$d\tilde{X}_t^d = \Gamma^d s_\theta^d(t, \tilde{X}_t^d) dt + \sqrt{2\Gamma^d} \tilde{W}_t^d, \quad \tilde{X}_0^d \sim \tilde{\rho}_0^d,$$

with path measure $\tilde{\mathbb{Q}}^d$. Recall that $\epsilon_t^d(x) := \nabla \log \rho_t^d(x) - s_\theta^d(t, x)$.

By Lemma A.1,

$$\text{KL}(\mathbb{P}^{v,d} \| \tilde{\mathbb{Q}}^d) = \text{KL}(\rho_0^d \| \tilde{\rho}_0^d) + \frac{1}{4} \int_0^T \int \|\Gamma^{d,1/2}(v_t^d + \epsilon_t^d)(x)\|^2 d\rho_t^d(x) dt.$$

Using $\|a + b\|^2 \leq 2\|a\|^2 + 2\|b\|^2$, we obtain

$$\text{KL}(\mathbb{P}^{v,d} \parallel \tilde{\mathbb{Q}}^d) \leq \text{KL}(\rho_0^d \parallel \tilde{\rho}_0^d) + \frac{1}{2} \int_0^T \int \|\Gamma^d)^{1/2} v_t^d(x)\|^2 d\rho_t^d(x) dt + \frac{1}{2} \int_0^T \int \|\Gamma^d)^{1/2} \epsilon_t^d(x)\|^2 d\rho_t^d(x) dt.$$

Since v^d is chosen so that $\text{Law}_{\mathbb{P}^{v,d}}(X_t^d) = \rho_t^d$, the data-processing inequality yields $\text{KL}(\rho_\star^d \parallel \tilde{\rho}_T^{\text{ALD},d}) \leq \text{KL}(\mathbb{P}^{v,d} \parallel \tilde{\mathbb{Q}}^d)$. Hence

$$\text{KL}(\rho_\star^d \parallel \tilde{\rho}_T^{\text{ALD},d}) \leq \text{KL}(\rho_0^d \parallel \tilde{\rho}_0^d) + \frac{1}{2} \int_0^T \int \|\Gamma^d)^{1/2} v_t^d(x)\|^2 d\rho_t^d(x) dt + \frac{1}{2} \int_0^T \int \|\Gamma^d)^{1/2} \epsilon_t^d(x)\|^2 d\rho_t^d(x) dt.$$

Taking the infimum over all such v^d , which satisfy $\partial_t \rho_t^d = -\nabla \cdot (\rho_t^d \Gamma^d v_t^d)$, yields

$$\text{KL}(\rho_\star^d \parallel \tilde{\rho}_T^{\text{ALD},d}) \leq \mathcal{E}_{\text{init}}^d + \mathcal{E}_{\text{bias},T}^d + \mathcal{E}_{\text{score},T}^d,$$

where

$$\mathcal{E}_{\text{init}}^d := \text{KL}(\rho_0^d \parallel \tilde{\rho}_0^d), \quad \mathcal{E}_{\text{score},T}^d := \frac{1}{2} \int_0^T \int \|\Gamma^d)^{1/2} \epsilon_t^d(x)\|^2 d\rho_t^d(x) dt,$$

and

$$\mathcal{E}_{\text{bias},T}^d := \frac{1}{2} \inf_{v^d: \partial_t \rho_t^d = -\nabla \cdot (\rho_t^d \Gamma^d v_t^d)} \int_0^T \int \|\Gamma^d)^{1/2} v_t^d(x)\|^2 d\rho_t^d(x) dt.$$

B.2. Proof of Proposition 4.3

At $t = 0$,

$$\rho_0^d(x) = \sum_{i \in I} w_i \varphi_{i,0}^d(x), \quad \tilde{\rho}_0^d(x) = \sum_{i \in I} \tilde{w}_i \tilde{\varphi}_{i,0}^d(x),$$

where

$$\varphi_{i,0}^d = \mathcal{N}(m_i^d, \Sigma_i^d + C^d), \quad \tilde{\varphi}_{i,0}^d = \mathcal{N}(\tilde{m}_i^d, \tilde{\Sigma}_i + C^d).$$

We have

$$\text{KL}(\rho_0^d \parallel \tilde{\rho}_0^d) = \sum_{i \in I} w_i \mathbb{E}_{X \sim \varphi_{i,0}^d} \left[\log \frac{\sum_{i \in I} w_i \varphi_{i,0}^d(X)}{\sum_{i \in I} \tilde{w}_i \tilde{\varphi}_{i,0}^d(X)} \right].$$

Consider the unnormalized weights

$$\phi^d(i, x) = w_i \varphi_{i,0}^d(x), \quad \tilde{\phi}^d(i, x) = \tilde{w}_i \tilde{\varphi}_{i,0}^d(x).$$

Then by data-processing inequality,

$$\text{KL}(\rho_0^d \parallel \tilde{\rho}_0^d) \leq \text{KL}(\phi^d \parallel \tilde{\phi}^d) = \text{KL}(w \parallel \tilde{w}) + \sum_{i \in I} w_i \text{KL}(\varphi_{i,0}^d \parallel \tilde{\varphi}_{i,0}^d),$$

where

$$\text{KL}(w \parallel \tilde{w}) = \sum_{i \in I} w_i \log \frac{w_i}{\tilde{w}_i},$$

and each Gaussian-Gaussian KL is explicit:

$$\begin{aligned} & \text{KL}(\varphi_{i,0}^d \parallel \tilde{\varphi}_{i,0}^d) \\ &= \frac{1}{2} \left[\left\| (\tilde{\Sigma}_i^d + C^d)^{-1/2} (\tilde{m}_i^d - m_i^d) \right\|_2^2 \right. \\ & \quad \left. + \text{Tr} \left((\tilde{\Sigma}_i^d + C^d)^{-1/2} (\Sigma_i^d + C^d) (\tilde{\Sigma}_i^d + C^d)^{-1/2} - I - \log \left((\tilde{\Sigma}_i^d + C^d)^{-1/2} (\Sigma_i^d + C^d) (\tilde{\Sigma}_i^d + C^d)^{-1/2} \right) \right) \right]. \end{aligned}$$

Under the diagonal assumption,

$$\text{KL}(\varphi_{i,0}^d \parallel \tilde{\varphi}_{i,0}^d) = \frac{1}{2} \sum_{j=1}^d \left[\frac{\sigma_{ij} + \lambda_j}{\sigma_{ij} + \Delta\sigma_{ij} + \lambda_j} - 1 + \frac{(\Delta m_{ij})^2}{\sigma_{ij} + \Delta\sigma_{ij} + \lambda_j} + \log \left(\frac{\sigma_{ij} + \Delta\sigma_{ij} + \lambda_j}{\sigma_{ij} + \lambda_j} \right) \right].$$

B.3. Proof of Proposition 4.4

We work with the two annealed mixtures ρ_t^d and $\tilde{\rho}_t^d$ introduced in the main text. Set

$$\Sigma_{i,t}^d := \Sigma_i^d + \kappa_t C^d, \quad \tilde{\Sigma}_{i,t}^d := \tilde{\Sigma}_i^d + \kappa_t C^d,$$

where $\kappa_t := (T - t)/T \in [0, 1]$. By Assumption 4.2 in the main text,

$$C^d = \text{Diag}(\lambda_j)_{j=1}^d, \quad \Gamma^d = \text{Diag}(\gamma_j)_{j=1}^d, \quad \Sigma_i^d = \text{Diag}(\sigma_{ij})_{j=1}^d, \quad \tilde{\Sigma}_i^d = \text{Diag}(\sigma_{ij} + \Delta\sigma_{ij})_{j=1}^d,$$

and therefore

$$\Sigma_{i,t}^d = \text{Diag}(\sigma_{ij} + \kappa_t \lambda_j)_{j=1}^d, \quad \tilde{\Sigma}_{i,t}^d = \text{Diag}(\sigma_{ij} + \Delta\sigma_{ij} + \kappa_t \lambda_j)_{j=1}^d.$$

We denote the (true and perturbed) component densities by

$$\varphi_{i,t}^d := \mathcal{N}(m_i^d, \Sigma_{i,t}^d), \quad \tilde{\varphi}_{i,t}^d := \mathcal{N}(\tilde{m}_i^d, \tilde{\Sigma}_{i,t}^d),$$

with $\tilde{m}_i^d = m_i^d + \Delta m_i^d$, so that

$$\rho_t^d(x) = \sum_{i \in I} w_i \varphi_{i,t}^d(x), \quad \tilde{\rho}_t^d(x) = \sum_{i \in I} \tilde{w}_i \tilde{\varphi}_{i,t}^d(x), \quad \sum_{i \in I} w_i = \sum_{i \in I} \tilde{w}_i = 1.$$

The responsibilities and component scores are

$$p_{i,t}(x) := \frac{w_i \varphi_{i,t}^d(x)}{\rho_t^d(x)}, \quad \tilde{p}_{i,t}(x) := \frac{\tilde{w}_i \tilde{\varphi}_{i,t}^d(x)}{\tilde{\rho}_t^d(x)},$$

and

$$S_{i,t}^d(x) := -(\Sigma_{i,t}^d)^{-1}(x - m_i^d), \quad \tilde{S}_{i,t}^d(x) := -(\tilde{\Sigma}_{i,t}^d)^{-1}(x - \tilde{m}_i^d).$$

With this notation,

$$\nabla \log \rho_t^d(x) = \sum_{i \in I} p_{i,t}(x) S_{i,t}^d(x), \quad \nabla \log \tilde{\rho}_t^d(x) = \sum_{i \in I} \tilde{p}_{i,t}(x) \tilde{S}_{i,t}^d(x),$$

and the score error $\epsilon_t^d := \nabla \log \tilde{\rho}_t^d - \nabla \log \rho_t^d$ decomposes as

$$\epsilon_t^d(x) = \underbrace{\sum_{i \in I} p_{i,t}(x) (\tilde{S}_{i,t}^d(x) - S_{i,t}^d(x))}_{=: I_1(x,t)} + \underbrace{\sum_{i \in I} (\tilde{p}_{i,t}(x) - p_{i,t}(x)) \tilde{S}_{i,t}^d(x)}_{=: I_2(x,t)}. \quad (27)$$

Hence proving Proposition 4.4 boils down to bounding the following two terms:

- (1) A component-score mismatch $\mathbb{E}_{\rho_t^d} [\|(\Gamma^d)^{1/2} I_1(X, t)\|^2]$.
- (2) A responsibility mismatch $\mathbb{E}_{\rho_t^d} [\|(\Gamma^d)^{1/2} I_2(X, t)\|^2]$.

(1) COMPONENT-SCORE MISMATCH: PROOF OF (18)

Define $\Delta S_{i,t}^d := \tilde{S}_{i,t}^d - S_{i,t}^d$. A direct expansion gives

$$\Delta S_{i,t}^d(x) = ((\Sigma_{i,t}^d)^{-1} - (\tilde{\Sigma}_{i,t}^d)^{-1})(x - m_i^d) + (\tilde{\Sigma}_{i,t}^d)^{-1}(\tilde{m}_i^d - m_i^d).$$

Let $\Delta m_i^d := \tilde{m}_i^d - m_i^d$ and write Δm_{ij} for its coordinates.

Using Jensen's inequality for the convex quadratic form $z \mapsto \|(\Gamma^d)^{1/2} z\|^2$ and $\sum_i p_{i,t}(x) = 1$,

$$\|(\Gamma^d)^{1/2} I_1(x, t)\|^2 = \left\| (\Gamma^d)^{1/2} \sum_{i \in I} p_{i,t}(x) \Delta S_{i,t}^d(x) \right\|^2 \leq \sum_{i \in I} p_{i,t}(x) \|(\Gamma^d)^{1/2} \Delta S_{i,t}^d(x)\|^2.$$

Integrating and using $\rho_t^d(x)p_{i,t}(x) = w_i\varphi_{i,t}^d(x)$ yields

$$\mathbb{E}_{\rho_t^d} [\|(\Gamma^d)^{1/2} I_1(X, t)\|^2] \leq \sum_{i \in I} w_i \int_{\mathbb{R}^d} \|(\Gamma^d)^{1/2} \Delta S_{i,t}^d(x)\|^2 \varphi_{i,t}^d(x) dx. \quad (28)$$

Using $(a+b)^2 \leq 2a^2 + 2b^2$,

$$\|(\Gamma^d)^{1/2} \Delta S_{i,t}^d(x)\|^2 \leq 2\|(\Gamma^d)^{1/2}((\Sigma_{i,t}^d)^{-1} - (\tilde{\Sigma}_{i,t}^d)^{-1})(x - m_i^d)\|^2 + 2\|(\Gamma^d)^{1/2}(\tilde{\Sigma}_{i,t}^d)^{-1} \Delta m_i^d\|^2.$$

Since everything is diagonal, the second term is explicit:

$$\|(\Gamma^d)^{1/2}(\tilde{\Sigma}_{i,t}^d)^{-1} \Delta m_i^d\|^2 = \sum_{j=1}^d \gamma_j \frac{(\Delta m_{ij})^2}{(\sigma_{ij} + \Delta\sigma_{ij} + \kappa_t \lambda_j)^2}.$$

For the first term, set

$$b_{ij}(t) := \frac{1}{\sigma_{ij} + \kappa_t \lambda_j} - \frac{1}{\sigma_{ij} + \Delta\sigma_{ij} + \kappa_t \lambda_j} = \frac{\Delta\sigma_{ij}}{(\sigma_{ij} + \kappa_t \lambda_j)(\sigma_{ij} + \Delta\sigma_{ij} + \kappa_t \lambda_j)},$$

so that $(\Sigma_{i,t}^d)^{-1} - (\tilde{\Sigma}_{i,t}^d)^{-1}$ has j -th diagonal entry $b_{ij}(t)$. Then

$$\|(\Gamma^d)^{1/2}((\Sigma_{i,t}^d)^{-1} - (\tilde{\Sigma}_{i,t}^d)^{-1})(x - m_i^d)\|^2 = \sum_{j=1}^d \gamma_j b_{ij}(t)^2 (x_j - m_{ij}^d)^2.$$

Since $\mathbb{E}[(X_j - m_{ij}^d)^2] = \sigma_{ij} + \kappa_t \lambda_j$ with $X \sim \mathcal{N}(m_i^d, \Sigma_{i,t}^d)$, we have

$$\int \|\Gamma^d)^{1/2}((\Sigma_{i,t}^d)^{-1} - (\tilde{\Sigma}_{i,t}^d)^{-1})(x - m_i^d)\|^2 \varphi_{i,t}^d(x) dx = \sum_{j=1}^d \gamma_j b_{ij}(t)^2 (\sigma_{ij} + \kappa_t \lambda_j) = \sum_{j=1}^d \gamma_j \frac{(\Delta\sigma_{ij})^2}{(\sigma_{ij} + \kappa_t \lambda_j)(\sigma_{ij} + \Delta\sigma_{ij} + \kappa_t \lambda_j)^2}.$$

Plugging everything into (28) gives

$$\mathbb{E}_{\rho_t^d} [\|(\Gamma^d)^{1/2} I_1(X, t)\|^2] \leq 2 \sum_{i \in I} w_i \sum_{j=1}^d \gamma_j \left[\frac{(\Delta m_{ij})^2}{(\sigma_{ij} + \Delta\sigma_{ij} + \kappa_t \lambda_j)^2} + \frac{(\Delta\sigma_{ij})^2}{(\sigma_{ij} + \kappa_t \lambda_j)(\sigma_{ij} + \Delta\sigma_{ij} + \kappa_t \lambda_j)^2} \right],$$

which is exactly (18) with

$$\mathbb{B}_{\text{comp}}^d(t) := 2 \sum_{i \in I} w_i \sum_{j=1}^d \gamma_j \frac{(\Delta m_{ij})^2 + \frac{(\Delta\sigma_{ij})^2}{\sigma_{ij} + \kappa_t \lambda_j}}{(\sigma_{ij} + \Delta\sigma_{ij} + \kappa_t \lambda_j)^2}.$$

This proves the first part of Proposition 4.4.

(2) RESPONSIBILITY MISMATCH: PROOF OF (19)

In this part it is convenient to abbreviate

$$\rho := \rho_t^d, \quad \tilde{\rho} := \tilde{\rho}_t^d, \quad \varphi_i := \varphi_{i,t}^d, \quad \tilde{\varphi}_i := \tilde{\varphi}_{i,t}^d, \quad \tilde{S}_i := \tilde{S}_{i,t}^d(\cdot), \quad p_i := p_{i,t}(\cdot), \quad \tilde{p}_i := \tilde{p}_{i,t}(\cdot).$$

Define also

$$\Delta w_i := \tilde{w}_i - w_i, \quad \Delta \varphi_i := \tilde{\varphi}_i - \varphi_i, \quad \Delta \rho := \tilde{\rho} - \rho.$$

A direct algebraic manipulation gives

$$\tilde{p}_i - p_i = \tilde{\varphi}_i \frac{\Delta w_i}{\tilde{\rho}} + w_i \frac{\Delta \varphi_i}{\tilde{\rho}} - w_i \varphi_i \frac{\Delta \rho}{\rho \tilde{\rho}}, \quad (29)$$

where

$$\Delta\rho(x) = \sum_{k \in I} \left[\Delta w_k \tilde{\varphi}_k(x) + w_k \Delta\varphi_k(x) \right]. \quad (30)$$

Correspondingly,

$$I_2(x, t) = \sum_{i \in I} (\tilde{p}_i - p_i)(x) \tilde{S}_i(x) = \delta^{(1)}(x) + \delta^{(2)}(x) + \delta^{(3)}(x),$$

with

$$\delta^{(1)}(x) := \sum_{i \in I} \tilde{\varphi}_i(x) \frac{\Delta w_i}{\tilde{\rho}(x)} \tilde{S}_i(x), \quad \delta^{(2)}(x) := \sum_{i \in I} w_i \frac{\Delta\varphi_i(x)}{\tilde{\rho}(x)} \tilde{S}_i(x), \quad \delta^{(3)}(x) := - \sum_{i \in I} w_i \varphi_i(x) \frac{\Delta\rho(x)}{\rho(x)\tilde{\rho}(x)} \tilde{S}_i(x). \quad (31)$$

Then

$$\mathbb{E}_\rho \left[\|(\Gamma^d)^{1/2} I_2(X, t)\|^2 \right] \leq 3 \sum_{r=1}^3 \mathbb{E}_\rho \left[\|(\Gamma^d)^{1/2} \delta^{(r)}(X)\|^2 \right]. \quad (32)$$

Using $p_i = w_i \varphi_i / \rho$ and (30),

$$\delta^{(3)}(x) = - \frac{\Delta\rho(x)}{\tilde{\rho}(x)} \sum_{i \in I} p_i(x) \tilde{S}_i(x) = - \left(\sum_{k \in I} \tilde{\varphi}_k(x) \frac{\Delta w_k}{\tilde{\rho}(x)} \right) J(x) - \left(\sum_{k \in I} w_k \frac{\Delta\varphi_k(x)}{\tilde{\rho}(x)} \right) J(x),$$

where

$$J(x) := \sum_{i \in I} p_i(x) \tilde{S}_i(x) \quad \text{is a convex combination of the vectors } \{\tilde{S}_i(x)\}_{i \in I}.$$

Thus $\delta^{(3)} = \delta^{(3,w)} + \delta^{(3,\varphi)}$, where the first term involves only the weight perturbations (Δw_k) and the second involves only the component-density perturbations ($\Delta\varphi_k$). Moreover, since $\sum_i p_i(x) = 1$ and $z \mapsto \|(\Gamma^d)^{1/2} z\|^2$ is convex,

$$\|(\Gamma^d)^{1/2} J(x)\|^2 \leq \sum_{i \in I} p_i(x) \|(\Gamma^d)^{1/2} \tilde{S}_i(x)\|^2. \quad (33)$$

Consequently, bounding $\delta^{(3,w)}$ uses the same input as bounding $\delta^{(1)}$ (weight perturbations times *second moments* of \tilde{S}_i), and bounding $\delta^{(3,\varphi)}$ uses the same input as bounding $\delta^{(2)}$ (component-density perturbations controlled through density ratios, as in the analysis below). For this reason, after defining the three terms in (31), it is enough to develop the bounds for $\delta^{(1)}$ and $\delta^{(2)}$ in detail: the term $\delta^{(3)}$ produces no new structural condition and can be absorbed into the same final upper bound by changing constants.

We now provide explicit bounds for $\delta^{(1)}$ and $\delta^{(2)}$ and then define a corresponding $B_{\text{resp}}^d(t)$.

(a) Weight perturbations: bound for $\delta^{(1)}$. Write $\tilde{S}_i(x) = -(\tilde{\Sigma}_{i,t}^d)^{-1}(x - \tilde{m}_i^d)$, hence

$$\|(\Gamma^d)^{1/2} \tilde{S}_i(x)\|^2 = \sum_{h=1}^d \gamma_h \frac{(x_h - \tilde{m}_{ih}^d)^2}{(\sigma_{ih} + \Delta\sigma_{ih} + \kappa_t \lambda_h)^2}.$$

Assume $\tilde{w}_i > 0$ for all $i \in I$, so that $\tilde{\rho}(x) \geq \tilde{w}_i \tilde{\varphi}_i(x)$. Fix $p \geq 2$ (we will take $p = 3$ below). We write

$$\delta^{(1)}(x) = \sum_{i \in I} \left(\frac{\Delta w_i}{\tilde{w}_i^{p/2}} \frac{\tilde{\varphi}_i(x)}{\tilde{\rho}(x)} \right) \tilde{w}_i^{p/2} \tilde{S}_i(x).$$

Cauchy–Schwarz yields

$$\|(\Gamma^d)^{1/2} \delta^{(1)}(x)\|^2 \leq \left(\sum_{i \in I} \frac{(\Delta w_i)^2}{\tilde{w}_i^p} \right) \sum_{i \in I} \tilde{w}_i^p \frac{\tilde{\varphi}_i(x)^2}{\tilde{\rho}(x)^2} \|(\Gamma^d)^{1/2} \tilde{S}_i(x)\|^2.$$

Using $\tilde{\rho}(x) \geq \tilde{w}_i \tilde{\varphi}_i(x)$, we get

$$\tilde{w}_i^p \frac{\tilde{\varphi}_i(x)^2}{\tilde{\rho}(x)^2} \leq \tilde{w}_i^p \frac{\tilde{\varphi}_i(x)^2}{\tilde{w}_i^2 \tilde{\varphi}_i(x)^2} = \tilde{w}_i^{p-2}.$$

Therefore

$$\|(\Gamma^d)^{1/2} \delta^{(1)}(x)\|^2 \leq \left(\sum_{i \in I} \frac{(\Delta w_i)^2}{\tilde{w}_i^p} \right) \sum_{i \in I} \tilde{w}_i^{p-2} \|(\Gamma^d)^{1/2} \tilde{S}_i(x)\|^2. \quad (34)$$

Integrating under ρ gives

$$\mathbb{E}_\rho [\|(\Gamma^d)^{1/2} \delta^{(1)}(X)\|^2] \leq \left(\sum_{i \in I} \frac{(\Delta w_i)^2}{\tilde{w}_i^p} \right) C_{d,p}^{(1)}(t), \quad (35)$$

where

$$C_{d,p}^{(1)}(t) := \int_{\mathbb{R}^d} \sum_{i \in I} \tilde{w}_i^{p-2} \|(\Gamma^d)^{1/2} \tilde{S}_i(x)\|^2 \rho(x) dx.$$

In particular, using $\rho = \sum_{\ell \in I} w_\ell \varphi_\ell$,

$$C_{d,p}^{(1)}(t) = \sum_{\ell \in I} w_\ell \sum_{i \in I} \tilde{w}_i^{p-2} \int_{\mathbb{R}^d} \|(\Gamma^d)^{1/2} \tilde{S}_i(x)\|^2 \varphi_\ell(x) dx.$$

If $X^{(\ell)} \sim \mathcal{N}(m_\ell^d, \Sigma_{\ell,t}^d)$, then for each coordinate h ,

$$\mathbb{E}[(X_h^{(\ell)} - \tilde{m}_{ih}^d)^2] = (\sigma_{\ell h} + \kappa_t \lambda_h) + (m_{\ell h}^d - \tilde{m}_{ih}^d)^2,$$

and hence

$$C_{d,p}^{(1)}(t) = \sum_{\ell \in I} w_\ell \sum_{i \in I} \tilde{w}_i^{p-2} \sum_{h=1}^d \gamma_h \frac{(\sigma_{\ell h} + \kappa_t \lambda_h) + (m_{\ell h}^d - \tilde{m}_{ih}^d)^2}{(\sigma_{ih} + \Delta \sigma_{ih} + \kappa_t \lambda_h)^2}. \quad (36)$$

Taking $p = 3$ yields the bound:

$$\mathbb{E}_\rho [\|(\Gamma^d)^{1/2} \delta^{(1)}(X)\|^2] \leq \left(\sum_{i \in I} \frac{(\Delta w_i)^2}{\tilde{w}_i^3} \right) \sum_{\ell \in I} w_\ell \sum_{i \in I} \tilde{w}_i \sum_{h=1}^d \gamma_h \frac{(\sigma_{\ell h} + \kappa_t \lambda_h) + (m_{\ell h}^d - \tilde{m}_{ih}^d)^2}{(\sigma_{ih} + \Delta \sigma_{ih} + \kappa_t \lambda_h)^2}.$$

(b) Component-density perturbations: bound for $\delta^{(2)}$. We now bound

$$\delta^{(2)}(x) = \sum_{i \in I} w_i \frac{\tilde{\varphi}_i(x) - \varphi_i(x)}{\tilde{\rho}(x)} \tilde{S}_i(x). \quad (37)$$

The key point is to avoid any factor depending on $|I|$ by repeatedly exploiting that responsibilities are convex weights.

Step 1: rewrite $\delta^{(2)}$ using $\tilde{\rho}$ -responsibilities. Define the $\tilde{\rho}$ -responsibilities

$$\tilde{\alpha}_i(x) := \frac{\tilde{w}_i \tilde{\varphi}_i(x)}{\tilde{\rho}(x)}.$$

Then $\tilde{\alpha}_i(x) \geq 0$ a.e., and (crucially, even for infinite mixtures)

$$\sum_{i \geq 1} \tilde{\alpha}_i(x) = \frac{\sum_{i \geq 1} \tilde{w}_i \tilde{\varphi}_i(x)}{\tilde{\rho}(x)} = \frac{\tilde{\rho}(x)}{\tilde{\rho}(x)} = 1 \quad \text{for a.e. } x.$$

Define the component density ratio and weight ratio

$$r_i(x) := \frac{\varphi_i(x)}{\tilde{\varphi}_i(x)}, \quad c_i := \frac{w_i}{\tilde{w}_i}.$$

Since $\tilde{\varphi}_i - \varphi_i = \tilde{\varphi}_i(1 - r_i)$,

$$w_i \frac{\tilde{\varphi}_i - \varphi_i}{\tilde{\rho}} = w_i \frac{\tilde{\varphi}_i}{\tilde{\rho}} (1 - r_i) = \frac{w_i}{\tilde{w}_i} \frac{\tilde{w}_i \tilde{\varphi}_i}{\tilde{\rho}} (1 - r_i) = \tilde{\alpha}_i(x) c_i (1 - r_i(x)).$$

Plugging into (37) yields the pointwise identity (a.e.)

$$\delta^{(2)}(x) = \sum_{i \geq 1} \tilde{\alpha}_i(x) c_i (1 - r_i(x)) \tilde{S}_i(x). \quad (38)$$

Step 2: pointwise convexity bound. Define for each i and a.e. x the vector

$$u_i(x) := c_i(1 - r_i(x)) (\Gamma^d)^{1/2} \tilde{S}_i(x).$$

Then (38) implies

$$(\Gamma^d)^{1/2} \delta^{(2)}(x) = \sum_{i \in I} \tilde{\alpha}_i(x) u_i(x).$$

Since $\sum_i \tilde{\alpha}_i(x) = 1$ and $\tilde{\alpha}_i(x) \geq 0$, we can apply Cauchy-Schwarz inequality and obtain:

$$\|(\Gamma^d)^{1/2} \delta^{(2)}(x)\|^2 \leq \sum_{i \in I} \tilde{\alpha}_i(x) \|u_i(x)\|^2 = \sum_{i \in I} \tilde{\alpha}_i(x) c_i^2 (1 - r_i(x))^2 \|(\Gamma^d)^{1/2} \tilde{S}_i(x)\|^2. \quad (39)$$

Step 3: change measure to $\tilde{\rho}$. Define the mixture density ratio

$$R(x) := \frac{\rho(x)}{\tilde{\rho}(x)}. \quad (40)$$

Then

$$\mathbb{E}_\rho \left[\|(\Gamma^d)^{1/2} \delta^{(2)}(X)\|^2 \right] = \mathbb{E}_{\tilde{\rho}} \left[R(X) \|(\Gamma^d)^{1/2} \delta^{(2)}(X)\|^2 \right].$$

By Cauchy-Schwarz,

$$\mathbb{E}_\rho \left[\|(\Gamma^d)^{1/2} \delta^{(2)}(X)\|^2 \right] \leq \left(\mathbb{E}_{\tilde{\rho}} [R(X)^2] \right)^{1/2} \left(\mathbb{E}_{\tilde{\rho}} \left[\|(\Gamma^d)^{1/2} \delta^{(2)}(X)\|^4 \right] \right)^{1/2}. \quad (41)$$

This step is valid whenever the two moments on the right are finite (otherwise the inequality remains true in $[0, \infty]$).

Step 4: bound the 4th moment. From (39), define a.e. in x the nonnegative functions

$$q_i(x) := c_i^2 (1 - r_i(x))^2 \|(\Gamma^d)^{1/2} \tilde{S}_i(x)\|^2, \quad Q(x) := \sum_{i \in I} \tilde{\alpha}_i(x) q_i(x).$$

By (39) we have $\|(\Gamma^d)^{1/2} \delta^{(2)}(x)\|^2 \leq Q(x)$, hence

$$\|(\Gamma^d)^{1/2} \delta^{(2)}(x)\|^4 \leq Q(x)^2. \quad (42)$$

Noting again that $\tilde{\alpha}_i(x) \geq 0$ and $\sum_i \tilde{\alpha}_i(x) = 1$, we can apply Cauchy-Schwarz inequality and obtain:

$$Q(x)^2 = \left(\sum_{i \in I} \tilde{\alpha}_i(x) q_i(x) \right)^2 \leq \sum_{i \in I} \tilde{\alpha}_i(x) q_i(x)^2.$$

Combine with (42):

$$\|(\Gamma^d)^{1/2} \delta^{(2)}(x)\|^4 \leq \sum_{i \in I} \tilde{\alpha}_i(x) c_i^4 (1 - r_i(x))^4 \|(\Gamma^d)^{1/2} \tilde{S}_i(x)\|^4.$$

Now integrate under $\tilde{\rho}$; since the integrand is nonnegative, Tonelli's theorem applies and allows exchanging sum and integral:

$$\begin{aligned}\mathbb{E}_{\tilde{\rho}}[\|(\Gamma^d)^{1/2}\delta^{(2)}(X)\|^4] &= \int \|(\Gamma^d)^{1/2}\delta^{(2)}(x)\|^4 \tilde{\rho}(x) dx \\ &\leq \int \sum_{i \in I} \tilde{\alpha}_i(x) c_i^4 (1 - r_i(x))^4 \|(\Gamma^d)^{1/2}\tilde{S}_i(x)\|^4 \tilde{\rho}(x) dx \\ &= \sum_{i \in I} \int \tilde{\alpha}_i(x) c_i^4 (1 - r_i(x))^4 \|(\Gamma^d)^{1/2}\tilde{S}_i(x)\|^4 \tilde{\rho}(x) dx.\end{aligned}$$

Use $\tilde{\alpha}_i = \tilde{w}_i \tilde{\varphi}_i / \tilde{\rho}$ to simplify each term:

$$\begin{aligned}\int \tilde{\alpha}_i(x) g(x) \tilde{\rho}(x) dx &= \int \frac{\tilde{w}_i \tilde{\varphi}_i(x)}{\tilde{\rho}(x)} g(x) \tilde{\rho}(x) dx \\ &= \tilde{w}_i \int g(x) \tilde{\varphi}_i(x) dx = \tilde{w}_i \mathbb{E}_{\tilde{\varphi}_i}[g(X)].\end{aligned}$$

Apply this with $g(x) = c_i^4 (1 - r_i(x))^4 \|(\Gamma^d)^{1/2}\tilde{S}_i(x)\|^4$ to obtain

$$\mathbb{E}_{\tilde{\rho}}[\|(\Gamma^d)^{1/2}\delta^{(2)}(X)\|^4] \leq \sum_{i \in I} \tilde{w}_i c_i^4 \mathbb{E}_{\tilde{\varphi}_i}[(1 - r_i(X))^4 \|(\Gamma^d)^{1/2}\tilde{S}_i(X)\|^4]. \quad (43)$$

To further bound (43), we introduce a useful lemma.

Lemma B.1. *For any $r > 0$,*

$$(1 - r)^4 \leq |\log r|^4 (r^4 + r^{-4}). \quad (44)$$

Proof. Let $\ell := \log r$ so $r = e^\ell$. By the mean value theorem for $f(u) = e^u$,

$$|e^\ell - 1| = |f(\ell) - f(0)| = |\ell| e^{\theta\ell} \quad \text{for some } \theta \in (0, 1).$$

Hence $e^{\theta\ell} \leq e^{|\ell|}$ and therefore

$$|1 - r| = |1 - e^\ell| \leq |\ell| e^{|\ell|}.$$

Raise both sides to the fourth power:

$$(1 - r)^4 \leq |\ell|^4 e^{4|\ell|}.$$

Now observe that for any real ℓ ,

$$e^{4|\ell|} = \max(e^{4\ell}, e^{-4\ell}) \leq e^{4\ell} + e^{-4\ell}.$$

Thus

$$(1 - r)^4 \leq |\ell|^4 (e^{4\ell} + e^{-4\ell}) = |\log r|^4 (r^4 + r^{-4}),$$

which is exactly (44). \square

Step 5: final bound. Apply Lemma B.1 with $r = r_i(X)$ and define

$$\ell_i(x) := \log r_i(x) = \log \frac{\varphi_i(x)}{\tilde{\varphi}_i(x)}.$$

Then pointwise (a.e.)

$$(1 - r_i(x))^4 \leq |\ell_i(x)|^4 (r_i(x)^4 + r_i(x)^{-4}).$$

Plug this into (43) to obtain

$$\mathbb{E}_{\tilde{\rho}}[\|(\Gamma^d)^{1/2}\delta^{(2)}(X)\|^4] \leq \sum_{i \geq 1} \tilde{w}_i c_i^4 \mathbb{E}_{\tilde{\varphi}_i} \left[|\ell_i(X)|^4 (r_i(X)^4 + r_i(X)^{-4}) \|(\Gamma^d)^{1/2}\tilde{S}_i(X)\|^4 \right]. \quad (45)$$

Combining (41) and (45) gives the explicit bound

$$\mathbb{E}_\rho \left[\|(\Gamma^d)^{1/2} \delta^{(2)}(X)\|^2 \right] \leq \left(\mathbb{E}_{\tilde{\rho}} [R(X)^2] \right)^{1/2} \left(\sum_{i \in I} \tilde{w}_i \left(\frac{w_i}{\tilde{w}_i} \right)^4 \mathbb{E}_{\tilde{\varphi}_i} \left[|\log r_i(X)|^4 (r_i(X)^4 + r_i(X)^{-4}) \|(\Gamma^d)^{1/2} \tilde{S}_i(X)\|^4 \right] \right)^{1/2}. \quad (46)$$

Finally, we further bound $E_{\tilde{\rho}}[R(X)^2]$. Using $\rho = \sum_k w_k \varphi_k$ and $\tilde{\rho} = \sum_k \tilde{w}_k \tilde{\varphi}_k$,

$$\begin{aligned} R(x) &= \frac{\rho(x)}{\tilde{\rho}(x)} = \sum_{k \geq 1} \frac{w_k \varphi_k(x)}{\tilde{\rho}(x)} = \sum_{k \geq 1} \frac{\tilde{w}_k \tilde{\varphi}_k(x)}{\tilde{\rho}(x)} \cdot \frac{w_k}{\tilde{w}_k} \cdot \frac{\varphi_k(x)}{\tilde{\varphi}_k(x)} \\ &= \sum_{k \geq 1} \tilde{\alpha}_k(x) c_k r_k(x). \end{aligned}$$

Noting again that $\tilde{\alpha}_k(x) \geq 0$ and $\sum_k \tilde{\alpha}_k(x) = 1$, we can apply Cauchy-Schwarz inequality and obtain:

$$R(x)^2 = \left(\sum_k \tilde{\alpha}_k(x) c_k r_k(x) \right)^2 \leq \sum_k \tilde{\alpha}_k(x) c_k^2 r_k(x)^2.$$

Now integrate under $\tilde{\rho}$; using Tonelli, we have

$$\mathbb{E}_{\tilde{\rho}}[R(X)^2] \leq \sum_{k \geq 1} \tilde{w}_k c_k^2 \mathbb{E}_{\tilde{\varphi}_k}[r_k(X)^2]. \quad (47)$$

(c) Explicit form of $\mathsf{B}_{\text{resp}}^d(t)$. Collect the bounds as follows. Define

$$\mathsf{B}_{\text{resp}}^d(t) := 3 \left(\mathsf{B}_{\text{w}}^d(t) + \mathsf{B}_{\varphi}^d(t) + \mathsf{B}_{\text{mix}}^d(t) \right),$$

where:

1. $\mathsf{B}_{\text{w}}^d(t)$ is any explicit upper bound for $\mathbb{E}_{\rho_t^d} \left[\|(\Gamma^d)^{1/2} \delta^{(1)}(X)\|^2 \right]$.
2. $\mathsf{B}_{\varphi}^d(t)$ is the right-hand side of (46).
3. $\mathsf{B}_{\text{mix}}^d(t)$ is a bound for the $\delta^{(3)}$ term in (32). As explained after (32), $\delta^{(3)} = \delta^{(3,w)} + \delta^{(3,\varphi)}$, and bounding $\delta^{(3,w)}$ uses the same weight perturbations as $\delta^{(1)}$ together with the convexity estimate (33), while bounding $\delta^{(3,\varphi)}$ uses the same component-density perturbations as $\delta^{(2)}$ (with \tilde{S}_i replaced by J , still controlled by (33)). Thus $\mathsf{B}_{\text{mix}}^d(t)$ can be taken to be a (slightly enlarged) combination of $\mathsf{B}_{\text{w}}^d(t)$ and $\mathsf{B}_{\varphi}^d(t)$, and in particular it introduces no additional condition beyond those already needed to make $\mathsf{B}_{\text{w}}^d(t)$ and $\mathsf{B}_{\varphi}^d(t)$ finite.

With this definition, (32) yields

$$\mathbb{E}_{\rho_t^d} \left\| \sum_{i \in I} (\tilde{p}_{i,t} - p_{i,t})(X) (\Gamma^d)^{1/2} \tilde{S}_{i,t}^d(X) \right\|^2 = \mathbb{E}_\rho \left[\|(\Gamma^d)^{1/2} I_2(X, t)\|^2 \right] \leq \mathsf{B}_{\text{resp}}^d(t),$$

which is (19). Together with the component bound already proved and (27), this implies

$$\mathcal{E}_{\text{score},T}^d \leq \int_0^T \left(\mathsf{B}_{\text{comp}}^d(t) + \mathsf{B}_{\text{resp}}^d(t) \right) dt,$$

which is (20) and completes the proof of Proposition 4.4.

B.4. Sufficient Conditions for (19) to Remain Uniform as $d \rightarrow \infty$

The bound (35) is dimension-free provided the following quantities remain bounded uniformly in d (and, when relevant, uniformly in i):

(W1) **Weight perturbations.** The weight-mismatch factor is uniformly bounded:

$$\sum_{i \in I} \frac{(\Delta w_i)^2}{\tilde{w}_i^3} < \infty.$$

(S1) **Preconditioner–variance compatibility.** The γ -weighted series appearing in (36) is uniformly bounded:

$$\sup_{d \geq 1} \sum_{\ell \in I} w_\ell \sum_{i \in I} \tilde{w}_i \sum_{h=1}^d \gamma_h \frac{(\sigma_{\ell h} + \kappa_t \lambda_h) + (m_{\ell h}^d - \tilde{m}_{ih}^d)^2}{(\sigma_{ih} + \Delta \sigma_{ih} + \kappa_t \lambda_h)^2} < \infty.$$

Obtaining a dimension-free version of (46) is more delicate, since it requires controlling, uniformly in d , several more involved quantities (and, when relevant, uniformly in i):

(W2) **Weights.** Uniform comparability of weights:

$$\sup_{i \in I} \frac{w_i}{\tilde{w}_i} < \infty \quad \text{and} \quad \sup_{i \in I} \frac{\tilde{w}_i}{w_i} < \infty.$$

This guarantees $\sum_i \tilde{w}_i (w_i/\tilde{w}_i)^4 \lesssim 1$.

(R2) **Mixture ratio second moment.** Since

$$\mathbb{E}_{\tilde{\rho}}[R(X)^2] \leq \sum_{k \geq 1} \tilde{w}_k c_k^2 \mathbb{E}_{\tilde{\varphi}_k}[r_k(X)^2],$$

a sufficient condition for $\mathbb{E}_{\tilde{\rho}}[R^2] < \infty$ is a uniform bound on $\mathbb{E}_{\tilde{\varphi}_i}[r_i^2]$. In the diagonal Gaussian case, we will show below that $\mathbb{E}_{\tilde{\varphi}_{ij}}[r_{ij}^2] < \infty$ iff $\tilde{v}_{ij} > \frac{1}{2}v_{ij}$; uniformity in d is then about the product over j , equivalently about summability of $\log \mathbb{E}_{\tilde{\varphi}_{ij}}[r_{ij}^2]$.

(Main) **Main term in (46).** The series

$$\sum_{i \in I} \tilde{w}_i \left(\frac{w_i}{\tilde{w}_i} \right)^4 \mathbb{E}_{\tilde{\varphi}_i} \left[|\log r_i(X)|^4 (r_i(X)^4 + r_i(X)^{-4}) \|(\Gamma^d)^{1/2} \tilde{S}_i(X)\|^4 \right]$$

must be bounded uniformly in d . In the diagonal Gaussian case, $\log r_i$ and $\|(\Gamma^d)^{1/2} \tilde{S}_i\|^2$ can be made explicit (see (50) and (51) below), so uniformity becomes an explicit summability/regularity statement involving (Δm_{ij}) , $(\Delta \sigma_{ij})$, and (γ_j) .

Since we already derived sufficient conditions for (19), we now focus on controlling (46). To this end, we make the dependence of the right-hand side of (46) explicit in terms of $w_i, \tilde{w}_i, m_{ij}, \tilde{m}_{ij}, \sigma_{ij}, \tilde{\sigma}_{ij}, \lambda_j$, and γ_j , in the same spirit as (36) for the bound on (19).

Define

$$v_{ij} := \sigma_{ij} + \kappa_t \lambda_j, \quad \tilde{v}_{ij} := \tilde{\sigma}_{ij} + \kappa_t \lambda_j = \sigma_{ij} + \Delta \sigma_{ij} + \kappa_t \lambda_j,$$

so that, for each component i ,

$$\tilde{\varphi}_i = \mathcal{N}(\tilde{m}_i, \tilde{\Sigma}_i), \quad \varphi_i = \mathcal{N}(m_i, \Sigma_i),$$

with diagonal covariances

$$\tilde{\Sigma}_i = \text{diag}(\tilde{v}_{ij})_{j=1}^d, \quad \Sigma_i = \text{diag}(v_{ij})_{j=1}^d, \quad \Gamma^d = \text{diag}(\gamma_j)_{j=1}^d.$$

Set the variance ratio

$$\kappa_{ij} := \frac{\tilde{v}_{ij}}{v_{ij}} = \frac{\sigma_{ij} + \Delta \sigma_{ij} + \kappa_t \lambda_j}{\sigma_{ij} + \kappa_t \lambda_j} = 1 + \frac{\Delta \sigma_{ij}}{v_{ij}}.$$

We make explicit two ingredients:

- (1) Uniformity in d for the mixture ratio second moment $\mathbb{E}_{\tilde{\rho}}[R^2]$.
- (2) Uniformity in d for the main term in (46), by completing the moment bounds into explicit summability conditions.

(1) UNIFORMITY IN d FOR $\mathbb{E}_{\tilde{\rho}}[R^2]$

Recall the bound already established:

$$\mathbb{E}_{\tilde{\rho}}[R(X)^2] \leq \sum_{i \geq 1} \tilde{w}_i c_i^2 \mathbb{E}_{\tilde{\varphi}_i}[r_i(X)^2], \quad c_i := \frac{w_i}{\tilde{w}_i}, \quad r_i(x) := \frac{\varphi_i(x)}{\tilde{\varphi}_i(x)}. \quad (48)$$

Write $x = (x_1, \dots, x_d)$. Then

$$\varphi_i(x) = \prod_{j=1}^d \frac{1}{\sqrt{2\pi v_{ij}}} \exp\left(-\frac{(x_j - m_{ij})^2}{2v_{ij}}\right), \quad \tilde{\varphi}_i(x) = \prod_{j=1}^d \frac{1}{\sqrt{2\pi \tilde{v}_{ij}}} \exp\left(-\frac{(x_j - \tilde{m}_{ij})^2}{2\tilde{v}_{ij}}\right),$$

hence

$$r_i(x) = \frac{\varphi_i(x)}{\tilde{\varphi}_i(x)} = \prod_{j=1}^d \left(\frac{\tilde{v}_{ij}}{v_{ij}}\right)^{1/2} \exp\left(-\frac{(x_j - m_{ij})^2}{2v_{ij}} + \frac{(x_j - \tilde{m}_{ij})^2}{2\tilde{v}_{ij}}\right). \quad (49)$$

Taking logs and using $x_j - m_{ij} = (x_j - \tilde{m}_{ij}) + \Delta m_{ij}$ yields

$$\begin{aligned} \ell_i(x) := \log r_i(x) &= \sum_{j=1}^d \left[\frac{1}{2} \log \frac{\tilde{v}_{ij}}{v_{ij}} - \frac{1}{2} \left(\frac{(x_j - m_{ij})^2}{v_{ij}} - \frac{(x_j - \tilde{m}_{ij})^2}{\tilde{v}_{ij}} \right) \right] \\ &= \sum_{j=1}^d \left[\underbrace{\frac{1}{2} \log \frac{\tilde{v}_{ij}}{v_{ij}} - \frac{(\Delta m_{ij})^2}{2v_{ij}}}_{=:c_{ij}} + \underbrace{\frac{1}{2} \left(\frac{1}{\tilde{v}_{ij}} - \frac{1}{v_{ij}} \right) (x_j - \tilde{m}_{ij})^2}_{=:a_{ij}^{(2)}} - \underbrace{\frac{\Delta m_{ij}}{v_{ij}} (x_j - \tilde{m}_{ij})}_{=:a_{ij}^{(1)}} \right]. \end{aligned} \quad (50)$$

Since $\tilde{S}_i(x) = -(\tilde{\Sigma}_i)^{-1}(x - \tilde{m}_i)$ and $\tilde{\Sigma}_i$ is diagonal,

$$(\tilde{S}_i(x))_j = -\frac{x_j - \tilde{m}_{ij}}{\tilde{v}_{ij}}, \quad \|(\Gamma^d)^{1/2} \tilde{S}_i(x)\|^2 = \sum_{j=1}^d \gamma_j \frac{(x_j - \tilde{m}_{ij})^2}{\tilde{v}_{ij}^2}. \quad (51)$$

So γ_j enters only through the weights γ_j multiplying $(x_j - \tilde{m}_{ij})^2/\tilde{v}_{ij}^2$.

Now, define

$$\tilde{\varphi}_{ij} := \mathcal{N}(\tilde{m}_{ij}, \tilde{v}_{ij}), \quad \varphi_{ij} := \mathcal{N}(m_{ij}, v_{ij}),$$

and

$$r_{ij}(x_j) := \varphi_{ij}(x_j)/\tilde{\varphi}_{ij}(x_j).$$

Then

$$\mathbb{E}_{\tilde{\varphi}_{ij}}[r_{ij}(X_j)^2] = \int_{\mathbb{R}} \frac{\varphi_{ij}(x_j)^2}{\tilde{\varphi}_{ij}(x_j)} dx_j.$$

We can write explicitly the probability density functions

$$\varphi_{ij}(x_j) = \frac{1}{\sqrt{2\pi v_{ij}}} \exp\left(-\frac{(x_j - m_{ij})^2}{2v_{ij}}\right), \quad \tilde{\varphi}_{ij}(x_j) = \frac{1}{\sqrt{2\pi \tilde{v}_{ij}}} \exp\left(-\frac{(x_j - \tilde{m}_{ij})^2}{2\tilde{v}_{ij}}\right).$$

Hence

$$\begin{aligned} \frac{\varphi_{ij}(x_j)^2}{\tilde{\varphi}_{ij}(x_j)} &= \left(\frac{1}{2\pi v_{ij}}\right) \sqrt{2\pi \tilde{v}_{ij}} \exp\left(-\frac{(x_j - m_{ij})^2}{v_{ij}} + \frac{(x_j - \tilde{m}_{ij})^2}{2\tilde{v}_{ij}}\right) \\ &= \frac{\sqrt{\tilde{v}_{ij}}}{v_{ij} \sqrt{2\pi}} \exp\left(-\frac{(x_j - m_{ij})^2}{v_{ij}} + \frac{(x_j - \tilde{m}_{ij})^2}{2\tilde{v}_{ij}}\right). \end{aligned}$$

We change variable $y_j := x_j - \tilde{m}_{ij}$ so that

$$x_j - m_{ij} = (x_j - \tilde{m}_{ij}) + (\tilde{m}_{ij} - m_{ij}) = y_j + \Delta m_{ij}.$$

Then

$$\begin{aligned} -\frac{(x_j - m_{ij})^2}{v_{ij}} + \frac{(x_j - \tilde{m}_{ij})^2}{2\tilde{v}_{ij}} &= -\frac{(y_j + \Delta m_{ij})^2}{v_{ij}} + \frac{y_j^2}{2\tilde{v}_{ij}} \\ &= -\left(\frac{1}{v_{ij}} - \frac{1}{2\tilde{v}_{ij}}\right)y_j^2 - \frac{2\Delta m_{ij}}{v_{ij}}y_j - \frac{(\Delta m_{ij})^2}{v_{ij}}. \end{aligned}$$

Set

$$A_{ij} := \frac{1}{v_{ij}} - \frac{1}{2\tilde{v}_{ij}} = \frac{2\tilde{v}_{ij} - v_{ij}}{2v_{ij}\tilde{v}_{ij}}.$$

The Gaussian integral is finite iff $A_{ij} > 0$, i.e. iff $2\tilde{v}_{ij} - v_{ij} > 0$ (equivalently $\tilde{v}_{ij} > v_{ij}/2$). Assuming $\tilde{v}_{ij} > v_{ij}/2$, we complete the square:

$$-A_{ij}y_j^2 - \frac{2\Delta m_{ij}}{v_{ij}}y_j = -A_{ij}\left(y_j + \frac{\Delta m_{ij}}{A_{ij}v_{ij}}\right)^2 + \frac{(\Delta m_{ij})^2}{A_{ij}v_{ij}^2}.$$

Therefore

$$-\frac{(y_j + \Delta m_{ij})^2}{v_{ij}} + \frac{y_j^2}{2\tilde{v}_{ij}} = -A_{ij}\left(y_j + \frac{\Delta m_{ij}}{A_{ij}v_{ij}}\right)^2 + \left(\frac{(\Delta m_{ij})^2}{A_{ij}v_{ij}^2} - \frac{(\Delta m_{ij})^2}{v_{ij}}\right).$$

We compute the constant:

$$\frac{(\Delta m_{ij})^2}{A_{ij}v_{ij}^2} - \frac{(\Delta m_{ij})^2}{v_{ij}} = (\Delta m_{ij})^2\left(\frac{1}{A_{ij}v_{ij}^2} - \frac{1}{v_{ij}}\right) = (\Delta m_{ij})^2 \cdot \frac{1 - A_{ij}v_{ij}}{A_{ij}v_{ij}^2}.$$

But $A_{ij}v_{ij} = \frac{2\tilde{v}_{ij} - v_{ij}}{2\tilde{v}_{ij}}$, so $1 - A_{ij}v_{ij} = \frac{v_{ij}}{2\tilde{v}_{ij}}$. Hence

$$\frac{1 - A_{ij}v_{ij}}{A_{ij}v_{ij}^2} = \frac{v_{ij}}{2\tilde{v}_{ij}} \cdot \frac{1}{A_{ij}v_{ij}^2} = \frac{1}{2\tilde{v}_{ij}} \cdot \frac{1}{A_{ij}v_{ij}} = \frac{1}{2\tilde{v}_{ij}} \cdot \frac{2\tilde{v}_{ij}}{2\tilde{v}_{ij} - v_{ij}} = \frac{1}{2\tilde{v}_{ij} - v_{ij}},$$

and thus the constant equals $(\Delta m_{ij})^2/(2\tilde{v}_{ij} - v_{ij})$.

Now we integrate:

$$\begin{aligned} \mathbb{E}_{\tilde{\varphi}_{ij}}[r_{ij}(X_j)^2] &= \frac{\sqrt{\tilde{v}_{ij}}}{v_{ij}\sqrt{2\pi}} \int_{\mathbb{R}} \exp\left(-A_{ij}\left(y_j + \frac{\Delta m_{ij}}{A_{ij}v_{ij}}\right)^2 + \frac{(\Delta m_{ij})^2}{2\tilde{v}_{ij} - v_{ij}}\right) dy_j \\ &= \frac{\sqrt{\tilde{v}_{ij}}}{v_{ij}\sqrt{2\pi}} \exp\left(\frac{(\Delta m_{ij})^2}{2\tilde{v}_{ij} - v_{ij}}\right) \int_{\mathbb{R}} \exp\left(-A_{ij}\left(y_j + \frac{\Delta m_{ij}}{A_{ij}v_{ij}}\right)^2\right) dy_j \\ &= \frac{\sqrt{\tilde{v}_{ij}}}{v_{ij}\sqrt{2\pi}} \exp\left(\frac{(\Delta m_{ij})^2}{2\tilde{v}_{ij} - v_{ij}}\right) \sqrt{\frac{\pi}{A_{ij}}}. \end{aligned}$$

We use $A_{ij} = (2\tilde{v}_{ij} - v_{ij})/(2v_{ij}\tilde{v}_{ij})$:

$$\frac{\sqrt{\tilde{v}_{ij}}}{v_{ij}\sqrt{2\pi}} \sqrt{\frac{\pi}{A_{ij}}} = \frac{\sqrt{\tilde{v}_{ij}}}{v_{ij}} \cdot \frac{1}{\sqrt{2A_{ij}}} = \frac{\sqrt{\tilde{v}_{ij}}}{v_{ij}} \sqrt{\frac{v_{ij}\tilde{v}_{ij}}{2\tilde{v}_{ij} - v_{ij}}} = \left(\frac{\tilde{v}_{ij}}{v_{ij}}\right) \frac{1}{\sqrt{2\tilde{v}_{ij}/v_{ij} - 1}}.$$

So finally

$$\mathbb{E}_{\tilde{\varphi}_{ij}}[r_{ij}(X_j)^2] = \left(\frac{\tilde{v}_{ij}}{v_{ij}}\right) \frac{1}{\sqrt{2\tilde{v}_{ij}/v_{ij} - 1}} \exp\left(\frac{(\Delta m_{ij})^2}{2\tilde{v}_{ij} - v_{ij}}\right), \quad \text{valid iff } \tilde{v}_{ij} > \frac{v_{ij}}{2}, \quad (52)$$

and in our diagonal setting,

$$r_i(x) = \prod_{j=1}^d r_{ij}(x_j), \quad \mathbb{E}_{\tilde{\varphi}_i}[r_i(X)^2] = \prod_{j=1}^d \mathbb{E}_{\tilde{\varphi}_{ij}}[r_{ij}(X_j)^2], \quad (53)$$

because $\tilde{\varphi}_i$ factorizes and r_i factorizes across coordinates.

Define the 1D factors

$$a_{ij} := \mathbb{E}_{\tilde{\varphi}_{ij}}[r_{ij}(X_j)^2] \in (0, \infty].$$

Then (53) reads $\mathbb{E}_{\tilde{\varphi}_i}[r_i^2(X)] = \prod_{j=1}^d a_{ij}$.

Step 1: $a_{ij} \geq 1$ and why uniformity in d is equivalent to $\sum_j \log a_{ij} < \infty$. First observe that $a_{ij} \geq 1$ always (whenever $a_{ij} < \infty$): indeed, since $r_{ij} = \varphi_{ij}/\tilde{\varphi}_{ij}$ and $\tilde{\varphi}_{ij}$ is a probability density,

$$\mathbb{E}_{\tilde{\varphi}_{ij}}[r_{ij}(X_j)] = \int \frac{\varphi_{ij}(x)}{\tilde{\varphi}_{ij}(x)} \tilde{\varphi}_{ij}(x) dx = \int \varphi_{ij}(x) dx = 1.$$

By Cauchy–Schwarz,

$$1 = (\mathbb{E}_{\tilde{\varphi}_{ij}}[r_{ij}])^2 \leq \mathbb{E}_{\tilde{\varphi}_{ij}}[r_{ij}^2] \cdot \mathbb{E}_{\tilde{\varphi}_{ij}}[1^2] = a_{ij}.$$

Hence $a_{ij} \geq 1$ and thus $\log a_{ij} \geq 0$.

Now fix i and define the partial products

$$A_{i,d} := \prod_{j=1}^d a_{ij} \quad (\text{so } A_{i,d} = \mathbb{E}_{\tilde{\varphi}_i}[r_i^2]).$$

Taking logs,

$$\log A_{i,d} = \sum_{j=1}^d \log a_{ij}. \quad (54)$$

Since $\log a_{ij} \geq 0$, the partial sums in (54) are increasing in d . Therefore:

$$\sup_{d \geq 1} A_{i,d} < \infty \iff \sup_{d \geq 1} \log A_{i,d} < \infty \iff \sup_{d \geq 1} \sum_{j=1}^d \log a_{ij} < \infty \iff \sum_{j \geq 1} \log a_{ij} < \infty.$$

So, in the diagonal Gaussian case, *uniformity in d of $\mathbb{E}_{\tilde{\varphi}_i}[r_i^2]$ is equivalent to summability of $\sum_{j \geq 1} \log \mathbb{E}_{\tilde{\varphi}_{ij}}[r_{ij}^2]$.*

Step 2: explicit formula for a_{ij} and an explicit summability condition. Set

$$\Delta m_{ij} := \tilde{m}_{ij} - m_{ij}, \quad \Delta \sigma_{ij} := \tilde{\sigma}_{ij} - \sigma_{ij}, \quad \kappa_{ij} := \frac{\tilde{v}_{ij}}{v_{ij}}.$$

Recall that $a_{ij} < \infty$ iff $\kappa_{ij} > 1/2$ and in that case

$$a_{ij} = \mathbb{E}_{\tilde{\varphi}_{ij}}[r_{ij}^2] = \left(\frac{\tilde{v}_{ij}}{v_{ij}} \right) \frac{1}{\sqrt{2\tilde{v}_{ij}/v_{ij} - 1}} \exp\left(\frac{(\Delta m_{ij})^2}{2\tilde{v}_{ij} - v_{ij}} \right) = \frac{\kappa_{ij}}{\sqrt{2\kappa_{ij} - 1}} \exp\left(\frac{(\Delta m_{ij})^2}{v_{ij}(2\kappa_{ij} - 1)} \right). \quad (55)$$

Taking logs,

$$\log a_{ij} = \underbrace{\log \kappa_{ij} - \frac{1}{2} \log(2\kappa_{ij} - 1)}_{=: g(\kappa_{ij})} + \frac{(\Delta m_{ij})^2}{v_{ij}(2\kappa_{ij} - 1)}. \quad (56)$$

Step 3: bound $g(\kappa)$. Define

$$g(\kappa) := \log \kappa - \frac{1}{2} \log(2\kappa - 1), \quad \kappa > 1/2.$$

Then $g(1) = 0$ and a direct computation gives

$$g'(\kappa) = \frac{1}{\kappa} - \frac{1}{2\kappa - 1}, \quad g''(\kappa) = -\frac{1}{\kappa^2} + \frac{2}{(2\kappa - 1)^2}.$$

In particular, $g'(1) = 1 - 1 = 0$. Fix $\varepsilon \in (0, 1/2)$ and assume $\kappa \in [1 - \varepsilon, 1 + \varepsilon]$. Then $\kappa \geq 1 - \varepsilon$ and $2\kappa - 1 \geq 1 - 2\varepsilon$, so

$$|g''(\kappa)| \leq \frac{1}{(1 - \varepsilon)^2} + \frac{2}{(1 - 2\varepsilon)^2} =: C_g(\varepsilon) < \infty.$$

By Taylor's theorem (using $g(1) = g'(1) = 0$), for each such κ there exists ξ between 1 and κ such that

$$g(\kappa) = \frac{1}{2}g''(\xi)(\kappa - 1)^2,$$

hence the explicit bound

$$0 \leq g(\kappa) \leq \frac{1}{2}C_g(\varepsilon)(\kappa - 1)^2 \quad \text{for all } \kappa \in [1 - \varepsilon, 1 + \varepsilon]. \quad (57)$$

Notice that nonnegativity $g(\kappa) \geq 0$ is consistent with $a_{ij} \geq 1$ and (56).

Step 4: an explicit sufficient condition for uniformity of $\mathbb{E}_{\tilde{\rho}}[R^2]$. Assume there exists $\varepsilon \in (0, 1/2)$ such that for all i, j ,

$$\kappa_{ij} = \frac{\tilde{v}_{ij}}{v_{ij}} \in [1 - \varepsilon, 1 + \varepsilon]. \quad (58)$$

Then $2\kappa_{ij} - 1 \geq 1 - 2\varepsilon > 0$ and (56)–(57) imply

$$\log a_{ij} \leq \frac{1}{2}C_g(\varepsilon)(\kappa_{ij} - 1)^2 + \frac{1}{1 - 2\varepsilon} \frac{(\Delta m_{ij})^2}{v_{ij}}. \quad (59)$$

Therefore, for each i ,

$$\sum_{j \geq 1} \log a_{ij} < \infty \iff \sum_{j \geq 1} (\kappa_{ij} - 1)^2 < \infty \text{ and } \sum_{j \geq 1} \frac{(\Delta m_{ij})^2}{v_{ij}} < \infty.$$

In particular, the following *uniform-in-i* condition implies $\sup_{i \geq 1} \sup_{d \geq 1} \mathbb{E}_{\tilde{\varphi}_i}[r_i^2] < \infty$:

$$\text{There exists } \varepsilon \in (0, 1/2) \text{ such that (58) holds and } \sup_{i \geq 1} \sum_{j \geq 1} \left((\kappa_{ij} - 1)^2 + \frac{(\Delta m_{ij})^2}{v_{ij}} \right) < \infty. \quad (60)$$

Assume (W2) (uniform comparability of weights), i.e. $\sup_i c_i < \infty$. Then from (48) and $\sum_i \tilde{w}_i = 1$,

$$\mathbb{E}_{\tilde{\rho}}[R^2] \leq (\sup_i c_i^2) \sum_i \tilde{w}_i \mathbb{E}_{\tilde{\varphi}_i}[r_i^2] \leq (\sup_i c_i^2) \cdot \sup_i \mathbb{E}_{\tilde{\varphi}_i}[r_i^2].$$

Thus (60) implies

$$\sup_{d \geq 1} \mathbb{E}_{\tilde{\rho}}[R^2] < \infty. \quad (61)$$

(2) UNIFORMITY IN d FOR THE MAIN TERM IN (46)

Define the main term that appears in (46)

$$\text{Main}_d := \sum_{i \in I} \tilde{w}_i c_i^4 \mathbb{E}_{\tilde{\varphi}_i} \left[|\log r_i(X)|^4 (r_i(X)^4 + r_i(X)^{-4}) \|(\Gamma^d)^{1/2} \tilde{S}_i(X)\|^4 \right]. \quad (62)$$

We derive explicit sufficient conditions ensuring $\sup_d \text{Main}_d < \infty$.

Step 1: remove $|\log r|^4$ by absorbing it into higher likelihood-ratio moments. Let $y \in \mathbb{R}$. We use the elementary inequality: for $u \geq 0$,

$$u^4 \leq 4! e^u = 24e^u$$

Apply this with $u = |y|$. Then $|y|^4 \leq 24e^{|y|} \leq 24(e^y + e^{-y})$, so

$$|y|^4 \leq 24(e^y + e^{-y}) \quad \forall y \in \mathbb{R}.$$

Now set $y = \log r$. Then $e^y = r$ and $e^{-y} = r^{-1}$, hence

$$|\log r|^4 \leq 24(r + r^{-1}).$$

Multiply by $(r^4 + r^{-4})$:

$$|\log r|^4 (r^4 + r^{-4}) \leq 24(r + r^{-1})(r^4 + r^{-4}) = 24(r^5 + r^{-3} + r^{-5} + r^3) \leq 24(2 + 2r^8 + 2r^{-8}),$$

because for $r > 0$, $r^5 \leq 1 + r^8$ and $r^3 \leq 1 + r^8$ (and similarly for negative powers). Thus we have the explicit pointwise bound, for all $r > 0$,

$$|\log r|^4 (r^4 + r^{-4}) \leq C_\star (1 + r^8 + r^{-8}), \quad C_\star := 48. \quad (63)$$

Apply (63) to $r = r_i(X)$ inside (62):

$$\text{Main}_d \leq C_\star \sum_{i \geq 1} \tilde{w}_i c_i^4 \mathbb{E}_{\tilde{\varphi}_i} \left[(1 + r_i(X)^8 + r_i(X)^{-8}) \|(\Gamma^d)^{1/2} \tilde{S}_i(X)\|^4 \right]. \quad (64)$$

Therefore it suffices to control, uniformly in d , the three families of terms

$$\mathbb{E}_{\tilde{\varphi}_i} \left[\|(\Gamma^d)^{1/2} \tilde{S}_i\|^4 \right], \quad \mathbb{E}_{\tilde{\varphi}_i} \left[r_i^8 \|(\Gamma^d)^{1/2} \tilde{S}_i\|^4 \right], \quad \mathbb{E}_{\tilde{\varphi}_i} \left[r_i^{-8} \|(\Gamma^d)^{1/2} \tilde{S}_i\|^4 \right].$$

Step 2: explicit $\tilde{\varphi}_i$ -moment of the score. Under $\tilde{\varphi}_i$, the coordinates $Z_{ij} := X_j - \tilde{m}_{ij}$ are independent with $Z_{ij} \sim \mathcal{N}(0, \tilde{v}_{ij})$. Since $(\tilde{S}_i(X))_j = -(X_j - \tilde{m}_{ij})/\tilde{v}_{ij} = -Z_{ij}/\tilde{v}_{ij}$,

$$\|(\Gamma^d)^{1/2} \tilde{S}_i(X)\|^2 = \sum_{j=1}^d \gamma_j \frac{Z_{ij}^2}{\tilde{v}_{ij}^2}.$$

Define $A_{ij} := \gamma_j Z_{ij}^2 / \tilde{v}_{ij}^2 \geq 0$. Then

$$\|(\Gamma^d)^{1/2} \tilde{S}_i(X)\|^4 = \left(\sum_{j=1}^d A_{ij} \right)^2 = \sum_{j=1}^d A_{ij}^2 + 2 \sum_{1 \leq j < k \leq d} A_{ij} A_{ik}.$$

Using independence of $(Z_{ij})_j$, we have $\mathbb{E}[A_{ij} A_{ik}] = \mathbb{E}[A_{ij}] \mathbb{E}[A_{ik}]$ for $j \neq k$. Compute

$$\mathbb{E}[A_{ij}] = \gamma_j \frac{\mathbb{E}[Z_{ij}^2]}{\tilde{v}_{ij}^2} = \gamma_j \frac{\tilde{v}_{ij}}{\tilde{v}_{ij}^2} = \frac{\gamma_j}{\tilde{v}_{ij}}, \quad \mathbb{E}[A_{ij}^2] = \gamma_j^2 \frac{\mathbb{E}[Z_{ij}^4]}{\tilde{v}_{ij}^4} = \gamma_j^2 \frac{3\tilde{v}_{ij}^2}{\tilde{v}_{ij}^4} = \frac{3\gamma_j^2}{\tilde{v}_{ij}^2}.$$

Therefore,

$$\begin{aligned} \mathbb{E}_{\tilde{\varphi}_i} \left[\|(\Gamma^d)^{1/2} \tilde{S}_i(X)\|^4 \right] &= \sum_{j=1}^d \frac{3\gamma_j^2}{\tilde{v}_{ij}^2} + 2 \sum_{j < k} \frac{\gamma_j}{\tilde{v}_{ij}} \frac{\gamma_k}{\tilde{v}_{ik}} \\ &= \left(\sum_{j=1}^d \frac{\gamma_j}{\tilde{v}_{ij}} \right)^2 + 2 \sum_{j=1}^d \frac{\gamma_j^2}{\tilde{v}_{ij}^2}. \end{aligned} \quad (65)$$

This identity is fully explicit and already shows the role of γ_j : dimension-free control requires the series $\sum_j \gamma_j / \tilde{v}_{ij}$ and $\sum_j \gamma_j^2 / \tilde{v}_{ij}^2$ to remain bounded (uniformly in i).

Step 3: handle $r_i^{\pm 8}$ by introducing a tilted Gaussian measure. Fix any real p such that the moment

$$M_i^{(p)} := \mathbb{E}_{\tilde{\varphi}_i}[r_i(X)^p]$$

is finite, and define

$$\tilde{\varphi}_i^{(p)}(x) := \frac{r_i(x)^p \tilde{\varphi}_i(x)}{M_i^{(p)}}.$$

Then $\tilde{\varphi}_i^{(p)}$ is a probability density and, for any nonnegative measurable function F ,

$$\mathbb{E}_{\tilde{\varphi}_i}[r_i(X)^p F(X)] = M_i^{(p)} \mathbb{E}_{\tilde{\varphi}_i^{(p)}}[F(X)]. \quad (66)$$

We will use (66) with $p = \pm 8$ and $F(X) = \|(\Gamma^d)^{1/2} \tilde{S}_i(X)\|^4$.

Step 4: explicit 1D formula for $M_i^{(p)}$ and its dimension-free criterion (via $\sum \log$). Since $r_i = \prod_{j=1}^d r_{ij}$ and $\tilde{\varphi}_i$ factorizes, we have

$$M_i^{(p)} = \mathbb{E}_{\tilde{\varphi}_i}[r_i^p] = \prod_{j=1}^d M_{ij}^{(p)}, \quad M_{ij}^{(p)} := \mathbb{E}_{\tilde{\varphi}_{ij}}[r_{ij}^p].$$

A direct Gaussian integration gives, with $\kappa_{ij} = \tilde{v}_{ij}/v_{ij}$ and $\Delta m_{ij} = \tilde{m}_{ij} - m_{ij}$,

$$M_{ij}^{(p)} = \frac{\kappa_{ij}^{p/2}}{\sqrt{p\kappa_{ij} - (p-1)}} \exp\left(\frac{p(p-1)(\Delta m_{ij})^2}{2v_{ij}(p\kappa_{ij} - (p-1))}\right), \quad \text{valid iff } p\kappa_{ij} - (p-1) > 0. \quad (67)$$

For $p = 8$ this requires $\kappa_{ij} > 7/8$, and for $p = -8$ it requires $\kappa_{ij} < 9/8$. Hence finiteness of both $M_i^{(8)}$ and $M_i^{(-8)}$ is guaranteed by the uniform band

$$\exists \varepsilon \in (0, 1/8) \text{ s.t. } \kappa_{ij} \in [1 - \varepsilon, 1 + \varepsilon] \quad \forall i, j. \quad (68)$$

We have

$$M_i^{(p)} = \prod_{j=1}^d M_{ij}^{(p)}, \quad \log M_i^{(p)} = \sum_{j=1}^d \log M_{ij}^{(p)}.$$

For $p > 1$ (e.g. $p = 8$) one has $M_{ij}^{(p)} \geq 1$ (same Jensen/Cauchy argument as before), so uniformity in d of $M_i^{(8)}$ is again equivalent to summability of $\sum_j \log M_{ij}^{(8)}$. Similarly for $p = -8$ under the band (68) (in fact $M_{ij}^{(-8)} \geq 1$ as well).

Moreover, under the uniform band (68), the logarithm of (67) satisfies

$$\log M_{ij}^{(p)} = \frac{p}{2} \log \kappa_{ij} - \frac{1}{2} \log(p\kappa_{ij} - (p-1)) + \frac{p(p-1)}{2} \frac{\Delta m_{ij}^2}{v_{ij}(p\kappa_{ij} - (p-1))}. \quad (69)$$

Exactly as in Part (1), the first two terms in (69) have a second-order cancellation at $\kappa = 1$, so for each fixed $p \in \{8, -8\}$ there exists a constant $C_p(\varepsilon) < \infty$ such that

$$\log M_{ij}^{(p)} \leq C_p(\varepsilon) (\kappa_{ij} - 1)^2 + C_p(\varepsilon) \frac{\Delta m_{ij}^2}{v_{ij}} \quad \text{for all } i, j; \quad (70)$$

here the proof uses the same Taylor/second-derivative argument as in (57), plus $p\kappa_{ij} - (p-1) \geq 1 - p\varepsilon > 0$.

Therefore the same summability condition as (60) implies uniform boundedness of both $M_i^{(8)}$ and $M_i^{(-8)}$:

$$\begin{aligned} \sup_{i \geq 1} \sum_{j \geq 1} \left((\kappa_{ij} - 1)^2 + \frac{\Delta m_{ij}^2}{v_{ij}} \right) &< \infty \quad \text{plus (68)} \\ &\Downarrow \\ \sup_{i \geq 1} \sup_{d \geq 1} M_i^{(8)} &< \infty \quad \text{and} \quad \sup_{i \geq 1} \sup_{d \geq 1} M_i^{(-8)} < \infty. \end{aligned} \quad (71)$$

Step 5: explicit tilted Gaussian parameters. Fix p with $p\kappa_{ij} - (p-1) > 0$ and consider one coordinate j . Under $\tilde{\varphi}_{ij}^{(p)}$, the random variable X_j is Gaussian. Indeed, an explicit completion-of-squares computation shows that the probability density function $\tilde{\varphi}_{ij}^{(p)}$ of X_j is

$$\begin{aligned}\tilde{\varphi}_{ij}^{(p)}(x_j) &= \frac{1}{M_{ij}^{(p)}} r_{ij}(x_j)^p \tilde{\varphi}_{ij}(x_j) = \frac{1}{M_{ij}^{(p)}} \frac{\varphi_{ij}(x_j)^p}{\tilde{\varphi}_{ij}(x_j)^{p-1}} \\ &= \frac{1}{\sqrt{2\pi}} \frac{1}{M_{ij}^{(p)}} \frac{\tilde{v}_{ij}^{(p-1)/2}}{v_{ij}^{p/2}} \exp \left[-\frac{p(x_j - m_{ij})^2}{2v_{ij}} + \frac{(p-1)(x_j - \tilde{m}_{ij})^2}{2\tilde{v}_{ij}} \right] \\ &= \frac{1}{\sqrt{2\pi v_{ij}^{(p)}}} \exp \left[-\frac{(x_j - m_{ij}^{(p)})^2}{2v_{ij}^{(p)}} \right]\end{aligned}$$

with

$$v_{ij}^{(p)} = \frac{\tilde{v}_{ij}}{D_{ij}(p)}, \quad m_{ij}^{(p)} = \tilde{m}_{ij} - \frac{p\kappa_{ij}}{D_{ij}(p)} \Delta m_{ij}, \quad D_{ij}(p) := p\kappa_{ij} - (p-1), \quad (72)$$

which gives:

$$X_j \sim \mathcal{N}(m_{ij}^{(p)}, v_{ij}^{(p)}) \quad \text{under } \tilde{\varphi}_{ij}^{(p)}. \quad (73)$$

Consequently, if we set $Z_{ij} := X_j - \tilde{m}_{ij}$, then under $\tilde{\varphi}_{ij}^{(p)}$ we have

$$Z_{ij} \sim \mathcal{N}(\mu_{ij}^{(p)}, v_{ij}^{(p)}), \quad \mu_{ij}^{(p)} := -\frac{p\kappa_{ij}}{D_{ij}(p)} \Delta m_{ij}, \quad v_{ij}^{(p)} = \frac{\tilde{v}_{ij}}{D_{ij}(p)}.$$

Step 6: explicit bound for $\mathbb{E}_{\tilde{\varphi}_i^{(p)}}[\|(\Gamma^d)^{1/2} \tilde{S}_i\|^4]$. Under $\tilde{\varphi}_i^{(p)}$, coordinates remain independent (still diagonal). We again use $A_{ij} := \gamma_j Z_{ij}^2 / \tilde{v}_{ij}^2$ but now Z_{ij} has mean $\mu_{ij}^{(p)}$ and variance $v_{ij}^{(p)}$. As before,

$$\mathbb{E} \left[\left(\sum_{j=1}^d A_{ij} \right)^2 \right] = \sum_{j=1}^d \mathbb{E}[A_{ij}^2] + 2 \sum_{j < k} \mathbb{E}[A_{ij}] \mathbb{E}[A_{ik}] \leq \left(\sum_{j=1}^d \mathbb{E}[A_{ij}] \right)^2 + \sum_{j=1}^d \mathbb{E}[A_{ij}^2].$$

Compute, using Gaussian moment formulas:

$$\mathbb{E}[Z_{ij}^2] = v_{ij}^{(p)} + (\mu_{ij}^{(p)})^2, \quad \mathbb{E}[Z_{ij}^4] = 3(v_{ij}^{(p)})^2 + 6v_{ij}^{(p)}(\mu_{ij}^{(p)})^2 + (\mu_{ij}^{(p)})^4.$$

Thus

$$\mathbb{E}_{\tilde{\varphi}_i^{(p)}}[\|(\Gamma^d)^{1/2} \tilde{S}_i(X)\|^4] \leq \left(\sum_{j=1}^d \gamma_j \frac{v_{ij}^{(p)} + (\mu_{ij}^{(p)})^2}{\tilde{v}_{ij}^2} \right)^2 + \sum_{j=1}^d \gamma_j^2 \frac{3(v_{ij}^{(p)})^2 + 6v_{ij}^{(p)}(\mu_{ij}^{(p)})^2 + (\mu_{ij}^{(p)})^4}{\tilde{v}_{ij}^4}. \quad (74)$$

Now plug the explicit parameters (72) into (74). Since $v_{ij}^{(p)} = \tilde{v}_{ij}/D_{ij}(p)$ and $\mu_{ij}^{(p)} = -\frac{p\kappa_{ij}}{D_{ij}(p)} \Delta m_{ij}$, we obtain term-by-term:

$$\frac{v_{ij}^{(p)}}{\tilde{v}_{ij}^2} = \frac{1}{D_{ij}(p) \tilde{v}_{ij}}, \quad \frac{(\mu_{ij}^{(p)})^2}{\tilde{v}_{ij}^2} = \frac{p^2 \kappa_{ij}^2}{D_{ij}(p)^2} \frac{\Delta m_{ij}^2}{\tilde{v}_{ij}^2},$$

and

$$\frac{(v_{ij}^{(p)})^2}{\tilde{v}_{ij}^4} = \frac{1}{D_{ij}(p)^2} \frac{1}{\tilde{v}_{ij}^2}, \quad \frac{v_{ij}^{(p)}(\mu_{ij}^{(p)})^2}{\tilde{v}_{ij}^4} = \frac{p^2 \kappa_{ij}^2}{D_{ij}(p)^3} \frac{\Delta m_{ij}^2}{\tilde{v}_{ij}^3}, \quad \frac{(\mu_{ij}^{(p)})^4}{\tilde{v}_{ij}^4} = \frac{p^4 \kappa_{ij}^4}{D_{ij}(p)^4} \frac{\Delta m_{ij}^4}{\tilde{v}_{ij}^4}.$$

Hence (74) becomes

$$\begin{aligned}\mathbb{E}_{\tilde{\varphi}_i^{(p)}}[\|(\Gamma^d)^{1/2} \tilde{S}_i\|^4] &\leq \left(\sum_{j=1}^d \gamma_j \left[\frac{1}{D_{ij}(p) \tilde{v}_{ij}} + \frac{p^2 \kappa_{ij}^2}{D_{ij}(p)^2} \frac{\Delta m_{ij}^2}{\tilde{v}_{ij}^2} \right] \right)^2 \\ &\quad + \sum_{j=1}^d \gamma_j^2 \left[\frac{3}{D_{ij}(p)^2} \frac{1}{\tilde{v}_{ij}^2} + \frac{6p^2 \kappa_{ij}^2}{D_{ij}(p)^3} \frac{\Delta m_{ij}^2}{\tilde{v}_{ij}^3} + \frac{p^4 \kappa_{ij}^4}{D_{ij}(p)^4} \frac{\Delta m_{ij}^4}{\tilde{v}_{ij}^4} \right].\end{aligned} \quad (75)$$

Step 7: explicit dimension-free sufficient conditions for the main term in (46). Fix $\varepsilon \in (0, 1/8)$ and assume the band (68). Then for $p \in \{8, -8\}$, the denominators $D_{ij}(p) = p\kappa_{ij} - (p-1)$ satisfy uniform positive lower bounds:

$$D_{ij}(8) = 8\kappa_{ij} - 7 \geq 8(1 - \varepsilon) - 7 = 1 - 8\varepsilon > 0, \quad D_{ij}(-8) = 9 - 8\kappa_{ij} \geq 9 - 8(1 + \varepsilon) = 1 - 8\varepsilon > 0.$$

Also κ_{ij} is uniformly bounded above and below on the band.

Therefore, for each $p \in \{8, -8\}$ there exists a constant $C_p(\varepsilon) < \infty$ such that (75) implies the simpler bound

$$\mathbb{E}_{\tilde{\varphi}_i^{(p)}}[\|(\Gamma^d)^{1/2}\tilde{S}_i\|^4] \leq C_p(\varepsilon) \left(\left(\sum_{j=1}^d \frac{\gamma_j}{\tilde{v}_{ij}} \right)^2 + \left(\sum_{j=1}^d \gamma_j \frac{\Delta m_{ij}^2}{\tilde{v}_{ij}^2} \right)^2 + \sum_{j=1}^d \frac{\gamma_j^2}{\tilde{v}_{ij}^2} + \sum_{j=1}^d \gamma_j^2 \frac{\Delta m_{ij}^2}{\tilde{v}_{ij}^3} + \sum_{j=1}^d \gamma_j^2 \frac{\Delta m_{ij}^4}{\tilde{v}_{ij}^4} \right), \quad (76)$$

where we used that κ_{ij} and $D_{ij}(p)$ are bounded above/below, so they can be absorbed into $C_p(\varepsilon)$.

Now combine:

$$\mathbb{E}_{\tilde{\varphi}_i}[r_i^p \|(\Gamma^d)^{1/2}\tilde{S}_i\|^4] = M_i^{(p)} \mathbb{E}_{\tilde{\varphi}_i^{(p)}}[\|(\Gamma^d)^{1/2}\tilde{S}_i\|^4] \quad \text{by (66).}$$

Thus, using (64), a sufficient condition for $\sup_d \text{Main}_d < \infty$ is:

(M0) Uniform bound (in i and d) on $\mathbb{E}_{\tilde{\varphi}_i}[\|(\Gamma^d)^{1/2}\tilde{S}_i\|^4]$, which by (65) is ensured by

$$\sup_{i \geq 1} \sum_{j \geq 1} \frac{\gamma_j}{\tilde{v}_{ij}} < \infty \quad \text{and} \quad \sup_{i \geq 1} \sum_{j \geq 1} \frac{\gamma_j^2}{\tilde{v}_{ij}^2} < \infty. \quad (77)$$

(M \pm) Uniform bounds on $M_i^{(8)}$ and $M_i^{(-8)}$ (handled by (71)) together with uniform bounds on the tilted score 4th moments (handled by (76)), which is ensured by (68) plus:

$$\sup_{i \geq 1} \sum_{j \geq 1} \left((\kappa_{ij} - 1)^2 + \frac{\Delta m_{ij}^2}{v_{ij}} \right) < \infty \quad \text{and} \quad \sup_{i \geq 1} \sum_{j \geq 1} \gamma_j \frac{\Delta m_{ij}^2}{\tilde{v}_{ij}^2} < \infty, \quad (78)$$

and

$$\sup_{i \geq 1} \sum_{j \geq 1} \gamma_j^2 \frac{\Delta m_{ij}^2}{\tilde{v}_{ij}^3} < \infty, \quad \sup_{i \geq 1} \sum_{j \geq 1} \gamma_j^2 \frac{\Delta m_{ij}^4}{\tilde{v}_{ij}^4} < \infty, \quad (79)$$

together with (77).

(3) SUMMARY OF SUFFICIENT CONDITIONS FOR (46) TO STAY UNIFORM AS $d \rightarrow \infty$

We need to assume:

1. Uniform comparability of weights: $\sup_i \frac{w_i}{\tilde{w}_i}$ and $\sup_i \frac{\tilde{w}_i}{w_i} < \infty$.
2. The uniform variance-ratio band (68).
3. The summability (60) (this gives $\sup_d \mathbb{E}_{\tilde{\rho}}[R^2] < \infty$ and also uniform finiteness of $M_i^{(\pm 8)}$).
4. The preconditioner–covariance compatibility conditions (77), (78), (79).

Then all terms on the right-hand side of (64) are uniformly bounded in d , hence

$$\sup_{d \geq 1} \text{Main}_d < \infty.$$

Together with $\sup_{d \geq 1} \mathbb{E}_{\tilde{\rho}}[R^2] < \infty$, the bound (46) is uniformly bounded in d .

(4) THE ROLE OF THE PRECONDITIONER TO ACHIEVE UNIFORMITY IN d

All dimension-free requirements involving γ_j appear through the weighted series in (77)–(79). Concretely:

- Even in the ideal case $\Delta m_{ij} = 0$ (perfect mean match), dimension-free control of $\mathbb{E}[\|\Gamma^{1/2} \tilde{S}_i\|^4]$ already requires $\sum_j \gamma_j / \tilde{v}_{ij} < \infty$ and $\sum_j \gamma_j^2 / \tilde{v}_{ij}^2 < \infty$.
- When means mismatch, extra weighted summability is required, e.g. $\sum_j \gamma_j \Delta m_{ij}^2 / \tilde{v}_{ij}^2 < \infty$.

This is exactly the mechanism by which choosing γ_j sufficiently decaying (relative to \tilde{v}_{ij}) enforces dimension-free bounds.

C. Annealed Classifier Free Guidance

We have discussed annealing in the context of sampling from a target distribution via a forward diffusion by an appropriate choice of a time dependent drift. We remark here that annealing also may be useful in the context of Classifier Free Guidance when we also condition on a class label.

In order to relate to the above discussion we write the annealed Langevin diffusion in (4) as

$$dX_t^d = v(t, X_t^d) dt + \sqrt{2} dW_t^d, \quad t \in [0, T],$$

where we have chosen Γ^d to be the identity and we have

$$v(t, X) = \nabla \log \rho_t^d(X) = \nabla \log \left(\rho_\star^d * \mathcal{N}\left(0, \frac{T-t}{T} C^d\right) \right),$$

with ρ_\star^d the multimodal Gaussian mixture in (1). By appropriate choice of the time dependent drift via the selection of the time horizon T we can show that the distribution of X_T^d is close to ρ_\star^d in Kullback-Leibler (KL) divergence.

To contrast this with diffusion generative modeling consider p_t^d the distribution of Y^d for Y^d an Ornstein-Uhlenbeck process solving

$$dY_t^d = -Y_t^d dt + \sqrt{2} dW_t^d, \quad t \in [0, T],$$

with $p_0^d = \rho_\star^d$. Then for a Gaussian noise initial condition, $Y_0 \sim \mathcal{N}(0, \mathcal{I}^d)$, and Y^d solving in reverse time $\tau = T - t$ the SDE

$$dY_\tau^d = w(\tau, Y_\tau^d) d\tau + \sqrt{2} dW_\tau^d, \quad \tau \in [0, T],$$

one can show that for T large the distribution Y_T^d is close to ρ_\star^d for the choice

$$w(\tau, Y) = Y + 2S(\tau, Y)$$

with the score function defined by $S(\tau, Y) = \nabla \log p_{T-\tau}^d(Y)$ (Baldassari et al., 2023).

In Classifier Free Guidance (CFG) (Ho & Salimans, 2022) one considers conditional generation via conditioning on observation of a class label c and replace w by

$$w^{\text{CFG}}(\tau, Y) = Y + 2S^{\text{CFG}}(\tau, Y),$$

for

$$S^{\text{CFG}}(\tau, Y) = \nabla \log p_{T-\tau}^d(Y|c) + \omega (\nabla \log p_{T-\tau}^d(Y|c) - \nabla \log p_{T-\tau}^d(Y)).$$

Here ω is a ‘guidance scale’ and by increasing this one can generate samples more aligned with the data. In fact a relatively large guidance scale relaxation $\omega > 0$ is often considered. However, a large guidance scale steers the samples toward a high likelihood mode at the cost of reducing sample diversity and fidelity (Astolfi et al., 2024). It is clear that the distribution induced by CFG in general modifies the (conditional) target distribution and recent work shows in particular that in case of Gaussian mixtures in one and finite dimensions, it results in general in a sharper distribution than the target one (Bradley & Nakkiran, 2024; Pavasovic et al., 2025; Wu et al., 2024).

In order to improve the performance of CFG with a constant guidance scale recent works have considered annealing CFG where the guidance scale is chosen to be time dependent (Pavasovic et al., 2025; Yehezkel et al., 2025; Wang et al., 2024).

One may then start with a large guidance scale to promote rapid alignment with data and then reduce the guidance scale close to terminal time T to promote alignment with the target distribution. In this manner one can achieve both prompt alignment as well as high fidelity with the target distribution.

We remark also that in (Pavasovic et al., 2025) the authors discuss what they refer to as ‘blessing-of-dimensionality’ that in fact CFG generates samples with the right target distribution in the limit of high dimension d . They do this in the setting of a (centered) two mode gaussian mixture of equal strength, a setting analogous to the one we considered in the motivating example in the introduction, but with equal weights for the modes. In a first phase, up until what the authors refer to as a specification time the CFG correction serves to push the trajectory in the direction of the mean vector. After the specification time the effect of the CFG correction becomes negligible, in the limit of high dimension, thus explaining that CFG may generate high fidelity samples. The authors also introduce a power law form of the CFG score correction motivated by this observation and find that this improves fidelity and which effectively gives a time dependent guidance scale. In (Yehezkel et al., 2025) a learning algorithm is introduced to identify a time dependent score which also introduce an effective score that in general is nonlinear in the difference between the conditional and unconditional scores. Finally, in (Wang et al., 2024) various guidance scales that are only time dependent were considered and the authors found that the choice

$$\omega(\tau) = \omega_0 \left(\frac{T - \tau}{T} \right),$$

gave essentially the best performance among those tried. The annealing schedule for the classifier Free Guidance then starts with a simulation phase where the diffusion is driven toward the data distribution and with a monotonous predetermined tapering. This is analogous to the situation considered in this paper.

D. Further Details on the Experiments in Section 5

This appendix collects implementation details and additional diagnostics for the experiments of Section 5. All figures were generated in Google Colab (13GB RAM).

D.1. Targets

In the experiments of Section 5, the target at truncation level d is a two-component diagonal Gaussian mixture on \mathbb{R}^d ,

$$\rho_*^d = w_1 \mathcal{N}(m_1^d, \Sigma_1^d) + w_2 \mathcal{N}(m_2^d, \Sigma_2^d), \quad w = (0.75, 0.25),$$

with separated means $m_1^d = 0$ and $m_2^d = 10 e_1$ and diagonal covariances of the form $\Sigma_1^d = \tau_1 \Sigma^d$ and $\Sigma_2^d = \tau_2 \Sigma^d$. Throughout, Σ^d is built from a power-law spectrum: for a chosen exponent $\alpha_{\text{mix}} > 1$,

$$\Sigma^d = \text{Diag}(j^{-\alpha_{\text{mix}}})_{j=1}^d.$$

D.2. Implementation of preconditioned ALD

We implement preconditioned ALD for the experiments as an Euler–Maruyama discretization of the time-inhomogeneous diffusion

$$dX_t^d = \Gamma^d \nabla \log \rho_t^d(X_t^d) dt + \sqrt{2\Gamma^d} dW_t^d,$$

where $\Gamma^d = \text{Diag}(\gamma_j)_{j=1}^d$ is the diagonal preconditioner and ρ_t^d denotes the Gaussian-smoothed mixture along the annealing path. In discrete time, with stepsize Δt and N steps, the iteration is

$$X_{k+1}^d = X_k^d + \Delta t \Gamma^d s_{\theta_k}^d(X_k^d) + \sqrt{2\Delta t \Gamma^d} \xi_k^d, \quad \xi_k^d \sim \mathcal{N}(0, I_d),$$

where $s_{\theta}^d(x) = \nabla \log(\rho_*^d * \mathcal{N}(0, \theta C^d))(x)$ is the analytic score of the smoothed mixture at smoothing level θ and diagonal smoothing operator $C^d = \text{Diag}(\lambda_j)_{j=1}^d$.

We use the linear schedule

$$\theta_k = 2S \left(1 - \frac{k}{N-1} \right), \quad k = 0, \dots, N-1,$$

so $\theta_0 = 2S$ and $\theta_{N-1} = 0$. In the experiments: $S = 20$, $\Delta t = 9 \times 10^{-3}$, $N = 20000$, $T_{\text{cont}} := (N-1)\Delta t \approx 1.80 \times 10^2$.

D.3. ALD diffusion design choices: Γ^d and C^d

Both the preconditioner and smoothing are chosen as diagonal power laws (possibly up to constant factors),

$$\Gamma^d = \text{Diag}(\gamma_j)_{j=1}^d, \quad \gamma_j \propto j^{-\alpha_{\text{pre}}}, \quad C^d = \text{Diag}(\lambda_j)_{j=1}^d, \quad \lambda_j \propto j^{-\alpha_{\text{smooth}}}.$$

In Figure 3, we contrast two configurations:

$$(\Gamma^d, C^d) = (\text{Diag}(j^{-1.5})_{j=1}^d, \text{Diag}(j^{-2.7})_{j=1}^d), \quad (\Gamma^d, C^d) = (I_d, 40 I_d).$$

In Figure 4, we fix $C^d = \text{Diag}(j^{-4})_{j=1}^d$ and vary only the preconditioner:

$$\Gamma^d = \text{Diag}(j^{-3.5})_{j=1}^d, \quad \Gamma^d = \text{Diag}(j^{-1})_{j=1}^d,$$

so that one choice is consistent with the sufficient conditions used in the analysis while the other violates them.

D.4. Initialization choices

In Figure 3, we initialize from

$$X_0^d \sim (0.75) \mathcal{N}(m_1^d, \tau_1 \Sigma^d + C^d) + (0.25) \mathcal{N}(m_2^d, \tau_2 \Sigma^d + C^d),$$

with $C^d = \text{Diag}(40 \cdot j^{-2.7})_{j=1}^d$, $\tau_1 = 1.2$, $\tau_2 = 1$, and $\Sigma^d = \text{Diag}(j^{-1.25})_{j=1}^d$.

In Figure 4, to isolate the role of preconditioning under score error, we control initialization mismatch by perturbing only the mixture weights:

$$X_0^d \sim (0.1) \mathcal{N}(m_1^d, \Sigma^d) + (0.9) \mathcal{N}(m_2^d, \Sigma^d), \quad \Sigma^d = \text{Diag}(j^{-2})_{j=1}^d.$$

The component means and covariances are kept unchanged.

D.5. Score-error model in Figure 4: covariance-only perturbations

To simulate the score error while keeping the setting analytically transparent, we compute the drift using the *exact* score of a *misspecified* mixture where only the diagonal covariances are perturbed, while the weights and means remain unchanged. Concretely, if $\Sigma_i^d = \text{Diag}(\sigma_{ij})_{j=1}^d$, we set $\tilde{\Sigma}_i^d = \text{Diag}(\tilde{\sigma}_{ij})_{j=1}^d$ with $\tilde{\sigma}_{ij} = \sigma_{ij} + \Delta\sigma_{ij}$, where $\Delta\sigma_{ij}$ follows a power law $\Delta\sigma_{ij} \propto j^{-\alpha_{\text{err}}}$ with $\alpha_{\text{err}} = 3.5$. The ALD drift is then $\Gamma^d \nabla \log(\tilde{\rho}_*^d * \mathcal{N}(0, \theta C^d))$. This construction aligns with the error model of Section 4.

D.6. KL estimation via k NN

To estimate $\text{KL}(\rho_*^d \parallel \rho^{\text{ALD},d})$, we generate $n = 2500$ samples $X_1^{(p)}, \dots, X_n^{(p)} \sim \rho_*^d$ and $m = 2500$ samples $X_1^{(q)}, \dots, X_m^{(q)} \sim \rho^{\text{ALD},d}$, and apply a fixed- k nearest-neighbor estimator of $\text{KL}(P \parallel Q)$ (Pérez-Cruz, 2008; Wang et al., 2009). Below we report plots for $k \in \{20, 50, 80\}$ for both Figures 3 and 4 of the paper to confirm that the qualitative trends are robust with respect to the neighborhood size (the main text reports $k = 20$).

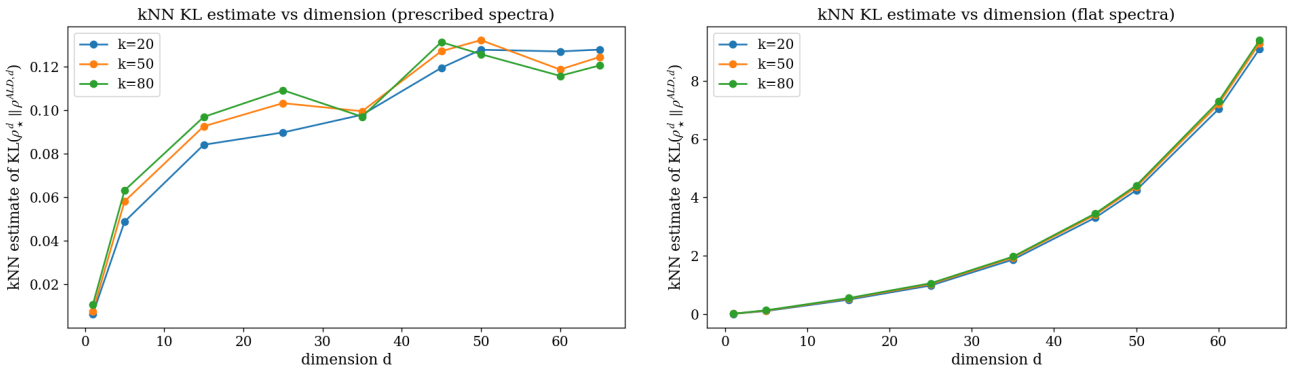


Figure 5. **Robustness to k .** Supplementary plots for Figure 3: we report the k NN estimate for $k \in \{20, 50, 80\}$ (the main text reports $k = 20$), illustrating that the observed trend is stable across these choices of k .

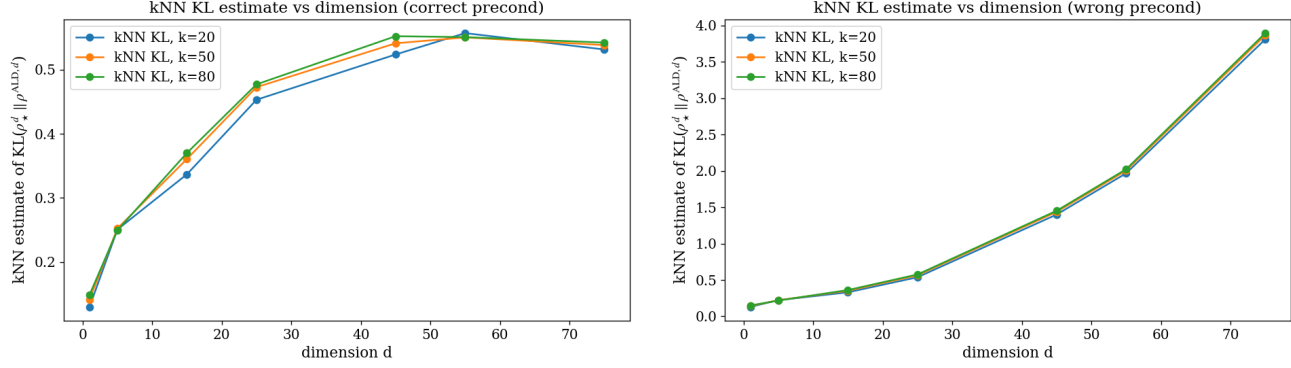


Figure 6. **Robustness to k .** Supplementary plots for Figure 4: we report the k NN estimate for $k \in \{20, 50, 80\}$ (the main text reports $k = 20$), illustrating that the observed trend is stable across these choices of k .